Accepted Manuscript

Structure-activity relationship studies on bax activator SMBA1 for the treatment of ER-Positive and triple-negative breast cancer

Gang Liu, Tao Yin, Hyejin Kim, Chunyong Ding, Zhuo Yu, Hong Wang, Haiying Chen, Ruping Yan, Eric A. Wold, Hao Zou, Xi Liu, Ye Ding, Qiang Shen, Jia Zhou

PII: S0223-5234(19)30521-5

DOI: https://doi.org/10.1016/j.ejmech.2019.06.004

Reference: EJMECH 11407

To appear in: *European Journal of Medicinal Chemistry*

Received Date: 22 March 2019

Revised Date: 16 May 2019

Accepted Date: 3 June 2019

Please cite this article as: G. Liu, T. Yin, H. Kim, C. Ding, Z. Yu, H. Wang, H. Chen, R. Yan, E.A. Wold, H. Zou, X. Liu, Y. Ding, Q. Shen, J. Zhou, Structure-activity relationship studies on bax activator SMBA1 for the treatment of ER-Positive and triple-negative breast cancer, *European Journal of Medicinal Chemistry* (2019), doi: https://doi.org/10.1016/j.ejmech.2019.06.004.

Graphic Abstract

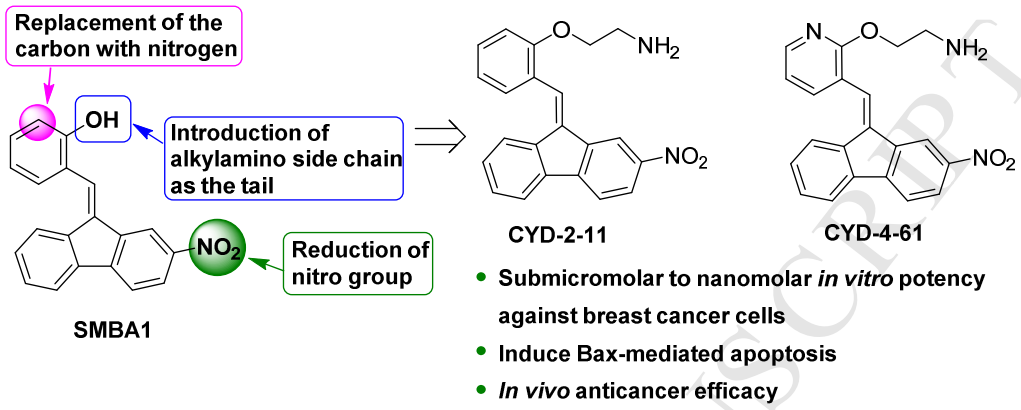

Structure-Activity Relationship Studies on Bax Activator SMBA1 for the Treatment of ER-Positive and Triple-Negative Breast Cancer

Gang Liu,[a,1] Tao Yin,[b,1] Hyejin Kim,[b] Chunyong Ding,[a] Zhuo Yu,[b] Hong Wang,[b] Haiying Chen,[a] Ruping Yan,[b] Eric A. Wold,[a] Hao Zou,[b] Xi Liu,[b] Ye Ding,[a] Qiang Shen[b,*] and Jia Zhou[a,*]

[a]*Chemical Biology Program, Department of Pharmacology and Toxicology, University of Texas Medical Branch, Galveston, Texas 77555, United States*

[b]*Department of Clinical Cancer Prevention, Division of Cancer Prevention and Population Sciences, The University of Texas MD Anderson Cancer Center, Houston, Texas 77030, United States*

[1]These authors contribute equally to this work.

***Corresponding authors:**

Jia Zhou, PhD
Chemical Biology Program
Department of Pharmacology and Toxicology
University of Texas Medical Branch
Galveston, Texas 77555, United States
Tel.: +1-409-772-9748
Email: jizhou@utmb.edu

Qiang Shen, PhD
Department of Clinical Cancer Prevention
Division of Cancer Prevention and Population Sciences
The University of Texas MD Anderson Cancer Center
Houston, Texas 77030, United States
Tel.: +1-713-834-6357
E-mail: qshen@mdanderson.org

Abstract

In an effort to develop novel Bax activators for breast cancer treatment, a series of diverse analogues have been designed and synthesized based on lead compound SMBA1 through several strategies, including introducing various alkylamino side chains to have a deeper access to S184 pocket, replacing carbon atoms with nitrogen, and reducing the nitro group of 9*H*-fluorene scaffold. Compounds **14** (CYD-2-11) and **49** (CYD-4-61) have been identified to exhibit significantly improved antiproliferative activity compared to SMBA1, with IC_{50} values of 3.22 μM and 0.07 μM against triple-negative breast cancer MDA-MB-231 and 3.81 μM and 0.06 μM against ER-positive breast cancer MCF-7 cell lines, respectively. Mechanism of action studies of compound **49** indicated that it can activate Bax protein to induce cytochrome *c* release and regulate apoptotic biomarkers, leading to cancer cell apoptosis. Further *in vivo* efficacy studies of compounds **14** and **49** in nude mice bearing MDA-MB-231 tumor xenografts demonstrated that these drug candidates can significantly suppress tumor growth, indicating their therapeutic potential for the treatment of breast cancer.

Keywords: Bax activator; SMBA1; S184; ER-Positive; Triple-Negative; Breast Cancer; Therapeutics.

Abbreviations

BC, breast cancer; HR, hormone receptor; ER, estrogen receptor; PR, progesterone receptor; TNBC, triple-negative breast cancer; SAR, structure-activity relationship; HTS, high-throughput screening; TLC, thin layer chromatography; UV, ultraviolet; TMS, tetramethylsilane; HRMS, high-resolution mass spectrometry; HPLC, high-performance liquid chromatography; DCM,

dichloromethane; EtOAc, ethyl acetate; DMSO, dimethyl sulfoxide; EDTA, ethylenediaminetetraacetic acid; DDT, dichlorodiphenyltrichloroethane; ADP, adenosine diphosphate;

1. Introduction

Breast cancer (BC) is currently the most prevalent malignant tumor and the leading cause of cancer-related death among women with 1.7 million cases and 521,900 deaths according to world-wide statistics reported for 2012 [1, 2]. Based on the American Cancer Society's estimate in 2018, nearly 12.4% of U.S. women will develop invasive breast cancer in their lifetimes and 266,120 new cases are expected to be diagnosed, including 40,920 fatal BC cases. Breast cancer can be generally classified into three subtypes according to the levels of hormone receptor (HR) and HER2 protein: (1) estrogen receptor (ER)-/progesterone receptor (PR)- positive type (~80%), (2) triple-negative type (10-15%), and (3) $HER2^+$ positive type (~5%) [3, 4]. The vast majority of common BC treatments include blocking hormone receptors or decreasing hormone levels through frontline medications, such as the HR blocker tamoxifen and aromatase inhibitors. Despite achieving a considerable overall response rate and decrease in mortality rates through single or combination therapeutic regimens for BC, side effects from these medications, such as bone mass loss, insomnia and others, create significant drawbacks during clinical use [5-8]. Due to the lack of well-defined molecular targeted drugs, triple-negative breast cancer (TNBC) is commonly treated with cytotoxic agents such as carboplatin, cisplatin and doxorubicin, which incur off-target toxicities and lack robust response in some patients [9-12]. In recent years, activated signaling pathways, such as ErbB, VEGF, Ras/MAPK, PI3K/Akt/mTOR, have been identified as molecular therapeutic targets for BC and have encouraged novel drug discovery efforts [13, 14]. However, drug resistance caused by protein mutations and failures to meet endpoints as single agents in clinically relevant, unselected patients has, in some cases, limited these therapeutics' applications [12, 15]. Taken together, new agents designed to treat BC with novel mechanisms of action are urgently needed to expand the available tools for clinical use.

Apoptosis has long been recognized as one of the major mechanisms of programmed cell death in response to cancer therapies [16, 17]. Certain cases of drug resistance and lack of efficacy for marketed drugs are due to the ability of malignant cells to evade drug-induced apoptosis [18]. Bax, an indispensable executioner protein of B-cell lymphoma 2 (Bcl-2) family, plays a pivotal role in regulating mitochondrial dysfunction and controlling apoptosis in normal and cancer cells [19]. Upon stimulation, it is transformed from an inactive cytosolic monomer into a lethal mitochondrial pore protein, inducing mitochondrial outer membrane permeabilization, the release of cytochrome *c*, and consequently inducing cancer cell apoptosis [20]. Accumulating evidence has shown that divergent levels of the active form of Bax and inactive form of Bax (i.e. pBax) are strongly correlated with various cancers such as melanoma [21, 22], non-small cell lung cancer [23, 24], and colon cancer [25]. Specifically in BC, significant downregulation of Bax has been observed and subsequent induction of Bax expression can restore its sensitivity to apoptotic stimuli [26-28]. Thus, Bax protein activation to induce cancer cell apoptosis represents an attractive strategy to inhibit cancer progression and combat drug resistance to available anticancer drugs.

To date, several classes of small molecules have been identified to selectively activate Bax to induce Bax-mediated apoptosis with micromolar to submicromolar *in vitro* activity and moderate *in vivo* activity by binding to different sites of Bax protein, such as *Zinc* 14750348 binding to Bax hydrophobic groove and BTC-8 interacting with Bax at the surface used by the BIM BH3 helix to trigger Bax (**Fig. 1**) [29-31]. In pursuit of novel small molecule Bax modulators with improved drug-likeness and a distinct binding site, our team sought to target the Ser184 phosphorylation site pocket as a potential ligand binding site and performed high throughput screening (HTS) using the NCI compound library, discovering the lead compound

SMBA1 as a Bax activator with 43 nM of binding affinity to Bax protein and promising *in vitro* and *in vivo* activity against lung cancer [32]. Intriguingly, further investigation using an SMBA1 derivative CYD-2-11 (**Fig. 1**) revealed that it not only displayed potent antitumor activity against KRAS-driven lung cancer *in vivo*, but also potentially overcame RAD001 resistance of lung cancer through restoring Bax activation [33]. The positive performance of these compounds in lung cancer directed our exploration into the therapeutic potential of SMBA1 and its structurally optimized analogues for BC treatment. Since our previous *in silico* docking analysis revealed that introducing an *O*-alkylamino side chain tethered to the hydroxyl group on the upper phenyl ring of lead compound SMBA1 could render deeper access into a binding pocket near S184 residue and improve Bax binding affinity [33], we decided to conduct a comprehensive medicinal chemistry campaign on the phenyl ring fragment by introducing various terminal linkers and replacing carbon atoms with nitrogen, as well as reducing the nitro group of the 9*H*-fluorene scaffold to construct a variety of SMBA1 analogues for SAR explorations (**Fig. 1**). Herein, we report the structural optimization of SMBA1 with a focus on improving the anticancer activity for BC treatment. These efforts led to the discovery of compound **14** (CYD-2-11) and **49** (CYD-4-61) (**Fig. 1**), two promising advanced chemical leads with significantly enhanced antiproliferative activity against breast cancer for further drug development.

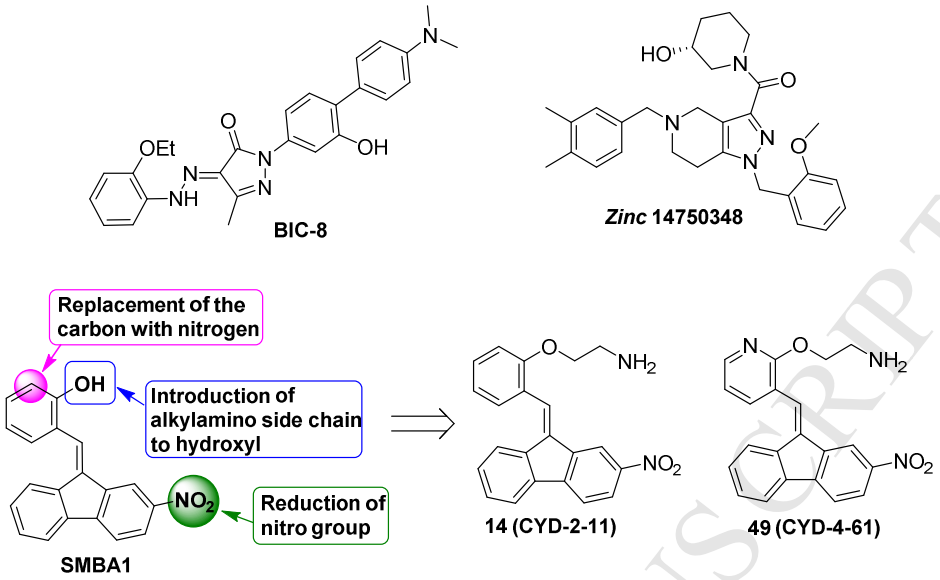

Fig. 1. Reported Bax activators and our molecular design.

2. Results and discussion

2.1 Chemistry

As outlined in **Scheme 1**, the diverse upper phenyl ring-substituted analogues were synthesized by condensation of 9*H*-fluorene **1** with various aldehydes that provided compounds as a mixture of *Z/E* isomer. The diastereoselectivity was determined by the appearance of two singlets around the chemical shift of 8.50 ppm, which were assigned to the proton signals of methylene next to nitro group on the fluorene ring. By condensation with commercially available 2-bromobenzaldehyde in the presence of KF-Al_2O_3 in MeOH [34], the 2-bromo analogue **2** was generated with 65:35 diastereomeric ratio in 53% yield. Coupling of **2** with diphenylmethanimine in the presence of $Pd_2(dba)_3$, BINAP, NaOtBu and PhMe [35], followed by hydrolysis of the resulting intermediate **3** afforded the final product **4** in 65% total yield (*dr*, 60:40). Compound **5** was obtained through coupling of **2** with N^1,N^1-dimethylethane-1,2-diamine following a similar condition as that for the preparation of **3** in 29% yield (*dr*, 65:35).

Condensation of **1** with 2-methoxybenzaldhyde or 2-hydroxybenzaldhyde provided compounds **6** (*dr*, 60:40) or **7** (**SMBA1** [32, 33], *dr*, 50:50) in a yield of 47% and 75%, respectively. Treatment of **7** with various amino alcohols in mitsunobu condition [36] afforded *O*-alkylamino substituted compounds **8** (*dr*, 50:50), **9** (*dr*, 50:50), **12** (*dr*, 50:50), **24** (*dr*, 55:45), **25** (*dr*, 50:50), **26** (*dr*, 55:45), and Boc-protected intermediates **10**, **13**, **16**, **18**, **20**, **22**, **27**, **32**, **34**, **36** in 51-86% yield. The Boc group in the latter intermediates were then deprotected with TFA to provide final compounds **11** (*dr*, 50:50), **14** (**CYD-2-11**, *dr*, 65:35), **17** (*dr*, 60:40), **19** (*dr*, 50:50), **21** (*dr*, 60:40), **23** (*dr*, 55:45), **28** (*dr*, 60:40), **33** (*dr*, 60:40), **35** (*dr*, 50:50), **37** (*dr*, 50:50) in 48-92% yields. Acetylation of **14** or **28** afforded amide compounds **15** (*dr*, 65:35) or **29** (*dr*, 50:50) in 83% and 77% yield, respectively. Meanwhile, ethylpiperazine **28** was converted into the methanesulfonamide **30** (*dr*, 60:40) or cyclopropanesulfonamide **31** (*dr*, 60:40) through the treatment with methylsulfonyl chloride or cyclopropanesulfonyl chloride, respectively, in 75-82% yields. It should be noted that to get chiral purity, we have successfully separated compound **14** into two single isomers by chiral HPLC with a baseline separation. However, interestingly, each of the single isomer could dynamically tautomerize to the opposite configuration and eventually reached an equilibrium mixture of both isomers, indicated by chiral HPLC analysis (data not shown).

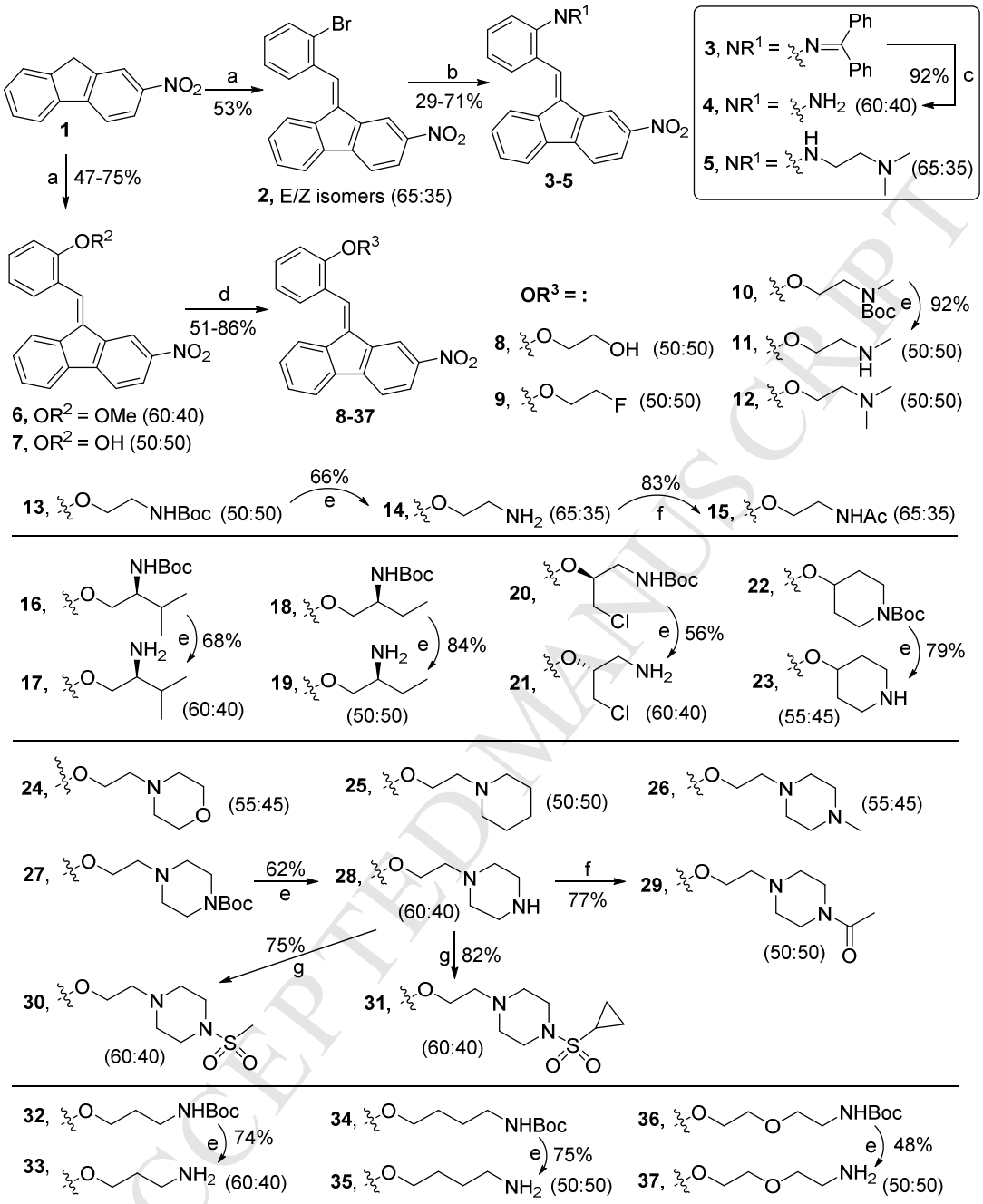

Scheme 1. Synthesis of compounds **4-37**. Reagents and conditions: (a) appropriate aldehyde, KF-Al_2O_3, MeOH, 65 ^oC, 16 h; (b) for **3**, diphenyl-methanimine, $Pd_2(dba)_3$, BINAP, NaO*t*Bu, PhMe, 110 ^oC, 18 h; for **5**, N^1,N^1-dimethylethane-1,2-diamine, $Pd_2(dba)_3$, BINAP, NaO*t*Bu, PhMe, 110 ^oC, 18 h; (c) 1 N HCl, THF, rt, 2 h; (d) for **8**, 2-bromoethan-1-ol, NaH, DMF, rt~80 ^oC, 24 h; for **9-37**, appropriate alcohols, Ph_3P, DIAD, THF, rt, 16 h; (e) TFA, CH_2Cl_2, rt, overnight; (f) acetyl chloride, Et_3N, CH_2Cl_2, rt, 18 h; (g) appropriate sulfonyl chlorides, Et_3N, CH_2Cl_2, rt, 4 h.

The synthesis of analogues with *O*-alkylamino side chain substituted at different positions or nitro reduction is described in **Scheme 2**. Treatment of hydroxybenzaldehydes with *tert*-butyl (2-hydroxyethyl)carbamate under Mitsunobu reaction conditions [36], followed by condensation with 9*H*-fluorene and subsequent TFA-assisted de-protection generated the final compound **41a** (*dr*, 50:50) or **41b** (*dr*, 50:50) in moderate yields. Reduction of the nitro group of **7** or **14** by zinc powder led to the corresponding aniline compounds **42** (*dr*, 65:35) or **43** (*dr*, 50:50) in 55% and 63% yield, respectively.

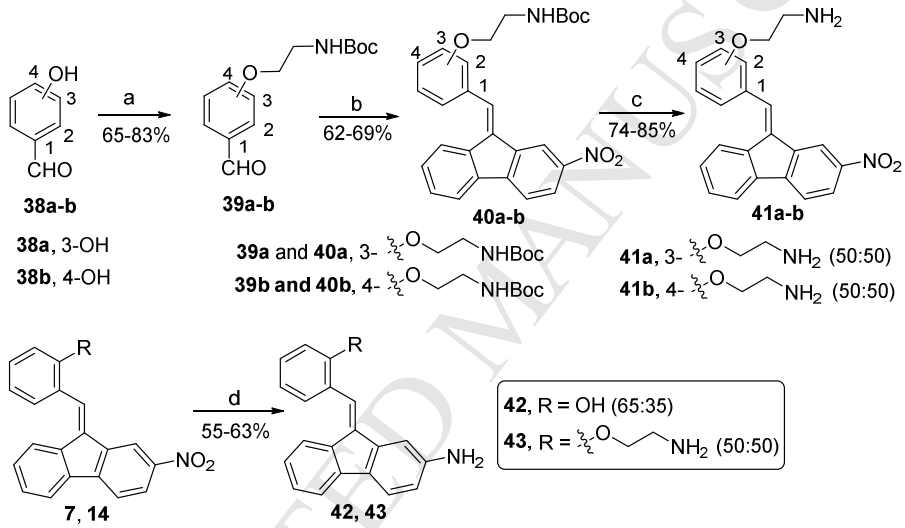

Scheme 2. Synthesis of compounds **41a-b** and **42-43**. Reagents and conditions: (a) *tert*-butyl (2-hydroxyethyl)carbamate, Ph_3P, DIAD, THF, rt, 16 h; (b) 9*H*-fluorene, KF-Al_2O_3, MeOH, 65 ^oC, 16 h; (c) TFA, CH_2Cl_2, rt, overnight; (d) Zn, NH_4Cl aq, THF, rt, 4 h.

Pyridyl-substituted analogues were synthesized as shown in **Scheme 3**. Treatment of 9*H*-fluorene **1** with hydroxyl-, methoxyl-pyridylaldehyde under standard condensation conditions [34] led to the corresponding compounds **44** (*dr*, 60:40), **45** (*dr*, 50:50) in 47-75% yield, respectively. Compound **47** (*dr*, 55:45) was obtained through a condensation, coupling and subsequent de-protection procedure following a similar method as the preparation of **4** in 23% overall yield. Condensation of *tert*-butyl (2-((3-formylpyridin-2-yl)oxy)ethyl)carbamate [37]

with **1** followed by removal of the Boc protecting group afforded compound **49** (**CYD-4-61**, *dr*, 50:50) in 52% overall yield. Similarly, compounds **50** (*dr*, 50:50) and **51** (*dr*, 55:45) were obtained through condensation of **1** with 2-(piperazin-1-yl)nicotinaldehyde [38] and 2-(4-methylpiperazin-1-yl)nicotinaldehyde [39], respectively.

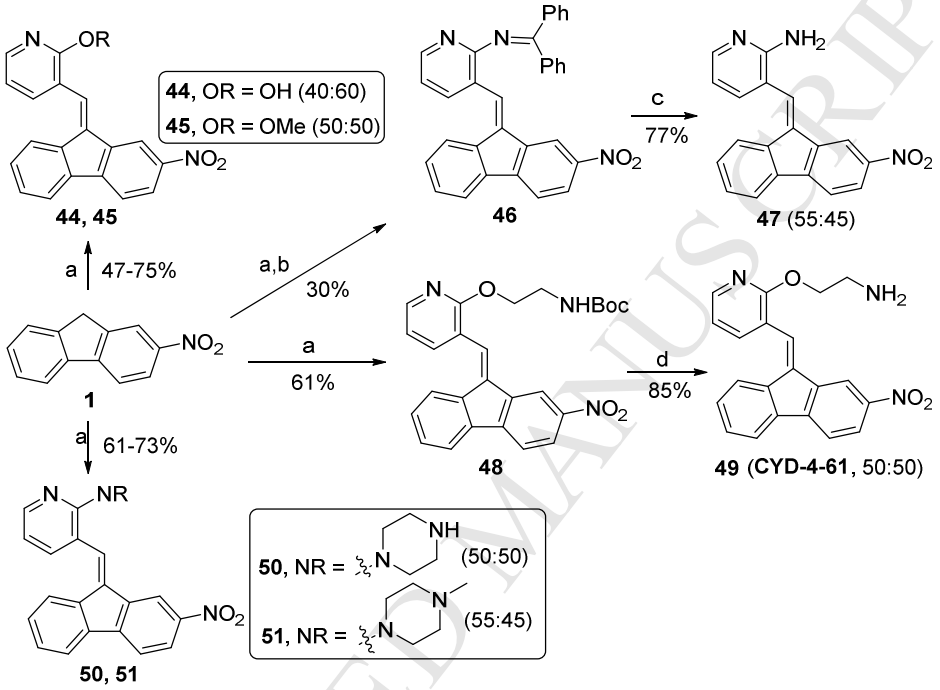

Scheme 3. Synthesis of compounds **44-45**, **47** and **49-51**. Reagents and conditions: (a) appropriate aldehyde, KF-Al_2O_3, MeOH, 65 ^oC, 16 h; (b) diphenylmethanimine, $Pd_2(dba)_3$, BINAP, NaO*t*Bu, PhMe, 110 ^oC, 18 h; (c) 1N HCl, THF, rt, 2 h; (d) TFA, CH_2Cl_2, rt, overnight.

2.2 Biology

2.2.1 Anti-proliferative Cellular Assay

Since lead compound **SMBA1**, reported to bind with an IC_{50} value of 43 nM to the S184 pocket of Bax protein [32], was previously observed to induce anti-breast cancer activity (**Table 1**), we decided to first determine the antiproliferative effects of our newly synthesized SMBA1 derivatives against breast cancer cells to identify new compounds with enhanced cell

permeability and anticancer activity. Two breast cancer cell lines MDA-MB-231 (triple-negative) and MCF-7 (ER-positive) were chosen for MTT assays using our established *in vitro* screening protocol [40]. IC_{50} values were further determined for those compounds showing inhibitory rates greater than 50% at the concentration of 10 μM. We first evaluated the antiproliferative effects of analogues with various terminal side chains in the upper phenyl ring, as summarized in **Table 1**. Replacement of terminal hydroxyl with a bromine, amino or methoxy moiety afforded compounds **2**, **4** or **6** and completely abolished the inhibitory activity. Further introducing a (*N*,*N*-dimethylamino)ethyl to **4** led to compound **5**, which has no obvious activity. Then various two-carbon side chains were introduced to the terminal hydroxyl of the upper ring in the parent compound. Hydroxyl ethyl (**8**) and fluoroethyl (**9**) ether analogues did not enhance the activity. Compound **11** with *N*-methylamino-ethyl as the side chain restored the antiproliferative effect with IC_{50} values of 5.48 μM and 4.26 μM against MDA-MB-231 and MCF-7, respectively. However, compound **12** containing (*N*,*N*-dimethylamino)ethyl fragment showed weak activity against MDA-MB-231, indicating the terminal N-H is critical for forming a hydrogen bond with the Bax protein in the S184 pocket [33]. Not surprisingly, compounds **13** and **15** with *N*-Boc and acetyl protected side chains exhibited negligible inhibitory activity, likely due to the lack of hydrogen bond forming capability. Notably, compound **14 (CYD-2-11**) with a free amino group at the tail significantly enhanced the anticancer potency with IC_{50} values of 3.22 μM and 3.81 μM against both MDA-MB-231 and MCF-7, respectively, which are 1.7 to 2.2-fold more potent than the lead compound SMBA1, as well as slightly more potent than **11**. Notable discrepancies were observed in the branched alkyl amino-containing compounds **17**, **19** and **21**, among which only compounds **17** and **19** retained good potency, whereas compound **21** with a chloroethyl substituent showed no activity at our testing concentrations. In addition, piperidine-containing

compound **23** was slightly less potent than **14**. These results suggest that both the two-carbon side chain and the basic hydrogen are important for the anticancer activity displayed by these compounds. Furthermore, morpholine, piperidine, piperazine and 1-methylpiperazine were incorporated into the tail of the two-carbon side chain leading to compounds **24-26** and **28**, which displayed much weaker potency overall except the piperazine analogue **28** with good potency of 3.5 µM and 4.97 µM. Consistent with the observation described earlier, acetylation or sulfonylation of **28** produced compounds **29-31** that displayed no activity, likely due to shielding the hydrogen bond formed by **28**. These results highlighted the critical contribution of the terminal basic amino pharmacophore in the side chain. Further, we evaluated the length of linker and found that all of the analogues with 3-carbon (**33**), 4-carbon (**35**) or PEG (**37**) linker showed slightly weaker activity against MDA-MB-231 and MCF-7 compared to **14**.

Table 1. The antiproliferative effects of analogues **2-37** against MDA-MB-231 and MCF-7 breast cancer cell lines.[a]

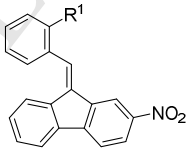

Entry	R^1	(IC_{50}, µM)		Entry	R^1	(IC_{50}, µM)	
		MDA-MB-231	MCF-7			MDA-MB-231	MCF-7
7 (SMBA1)		5.6 ± 0.69*	8.3 ± 1.44*	**19**	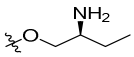	5.08 ± 0.19#	4.66 ± 0.95#
2		>10[b]	>10	**21**	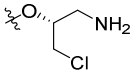	>10	>10
4		>10	>10	**23**	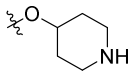	3.53 ± 0.3#	5.45 ± 0.12#

5	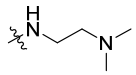	>10	>10	**24**	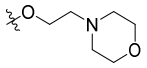	>10	ND[c]
6		>10	>10	**25**	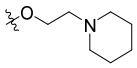	8.64 ± 3.38[#]	>10
8	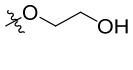	>10	ND	**26**	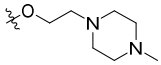	>10	9.58
9	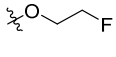	>10	>10	**28**	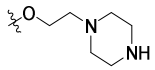	3.5 ± 0.23[#]	4.97 ± 0.46[#]
11	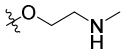	5.48 ± 0.65[#]	4.26 ± 0.89[#]	**29**	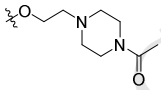	>10	>10
12	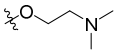	>10	>10	**30**	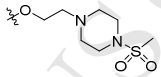	>10	ND
13	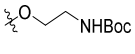	>10	>10	**31**	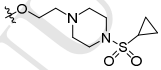	>10	ND
14	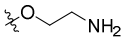	3.22 ± 0.49[*]	3.81 ± 0.76[*]	**33**	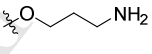	5.34 ± 0.81[#]	5.13
15	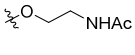	>10	>10	**35**	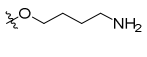	3.66 ± 1.71[#]	5.77 ± 0.77[#]
17	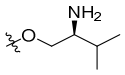	5.04 ± 0.07[#]	4.5 ± 0.59[#]	**37**	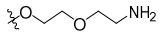	9.35 ± 2.48[#]	6.13 ± 1.48[#]

[a]Software: MasterPlex ReaderFit 2010, MiraiBio, Inc. [#]The values are the mean ±SD, and *values are the mean ±SE of at least three independent experiments. [b]If a specific compound is given a value >10, it indicates that a specific IC_{50} cannot be calculated from the data points collected, meaning 'no effect'. [c]ND – not determined.

The SAR study on the upper phenyl ring and the nitro group is summarized in **Table 2**. By taking advantage of the results shown in Table 1, we established the 2-aminoethyl as a privileged side chain and explored its location from 2- to 3- or 4-position on the phenyl ring, leading to compounds **41a-b** with slightly less potency compared to **14**. Compounds **42** and **43** can be viewed as the nitro reduction derivatives of compound **SMBA1** and **14**, respectively. Similarly, both of them exhibited minor activity decreases compared to their parental compounds. Replacement of the phenyl in SMBA1 with pyridyl afforded compound **44**, which was inactive

probably due to the tautomerism between 2-hydroxy pyridine and pyridone configuration. Further methoxy or amino substituted analogues **45** or **47** showed no obvious activity. Excitingly, incorporation of a 2-aminoethyl side chain into the pyridyl ring, in a similar strategy to that for the advanced chemical lead **14**, led to compound **49** (**CYD-4-61**), which exhibited significantly improved antiproliferative effects against both MDA-MB-231 and MCF-7 cancer cell lines with nanomolar IC_{50} values of 0.07 μM and 0.06 μM, respectively. Compound **49** was not only 80-130 fold more potent than the initial lead **SMBA1**, but also 40-60 fold more potent than the lead compound **14**. We further explored the 2-aminoethyl of **49** by replacement with piperazine or methylpiperazine to provide the terminally cyclized analogues **50** or **51**, respectively. Interestingly, compound **50** showed reduced anticancer potency (4.27 μM and 5 μM, respectively) compared to **49**, whereas compound **51** was completely inactive, indicating that the appropriate size and shape as well as the linker length of the side chain are important to form the key interactions within the S184 binding pocket of the Bax protein.

Table 2. The antiproliferative effects of new analogues **41-51** against MDA-MB-231 and MCF-7 breast cancer cell lines.[a]

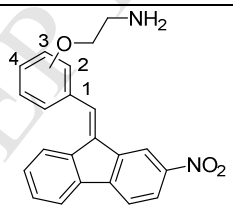

41a-b

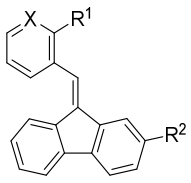

42-45, 47, 49-51

Entry	R^1	R^2	X	(IC_{50}, μM)	
				MDA-MB-231	MCF-7
41a	3 = 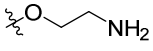			4.87 ± 0.58[#]	3.77
41b	4 = 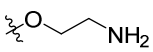			6.4 ± 0.46[#]	8.47 ± 0.56[#]

42	OH	NH_2	CH	>10	>10
43	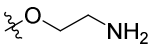	NH_2	CH	6.03 ± 2.35[#]	6.31
44	OH	NO_2	N	>10[b]	ND[c]
45	OMe	NO_2	N	>10	>10
47	NH_2	NO_2	N	>10	>10
49	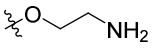	NO_2	N	0.07 ± 0.03[*]	0.06 ± 0.03[*]
50	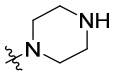	NO_2	N	4.27 ± 0.36[#]	5.0 ± 1.73[#]
51	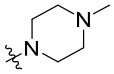	NO_2	N	>10	>10

[a]Software: MasterPlex ReaderFit 2010, MiraiBio, Inc. [#]The values are the mean ±SD, and *values are the mean ±SE of at least three independent experiments. [b]If a specific compound is given a value >10, it indicates that a specific IC_{50} cannot be calculated from the data points collected, meaning 'no effect'. [c]ND – not determined.

*2.2.2 Docking Analysis of Compound **49** (**CYD-4-61**) to Bax Protein.*

To investigate the possible binding mode of compound **49** to Bax protein and illustrate the significantly improved potency of **49**, we performed a virtual molecular docking study using the published solution structure of Bax (PDB ID: 1F16) and software Small Molecule Drug Discovery Suite 2019-1 (Schrödinger, LLC, New York, NY, 2019). As shown in **Fig. 2A-B**, the molecular docking analysis revealed that the introduced *O*-alkylamino side chain on the upper ring could form two hydrogen bonds with residue Asp102 around binding pocket near S184 site, which is consistent with our design. In addition, the nitrogen atom of the pyridine ring formed a hydrogen bond with residue Arg109, which was accounted for the better antiproliferative activity of compound **49** than **14**.

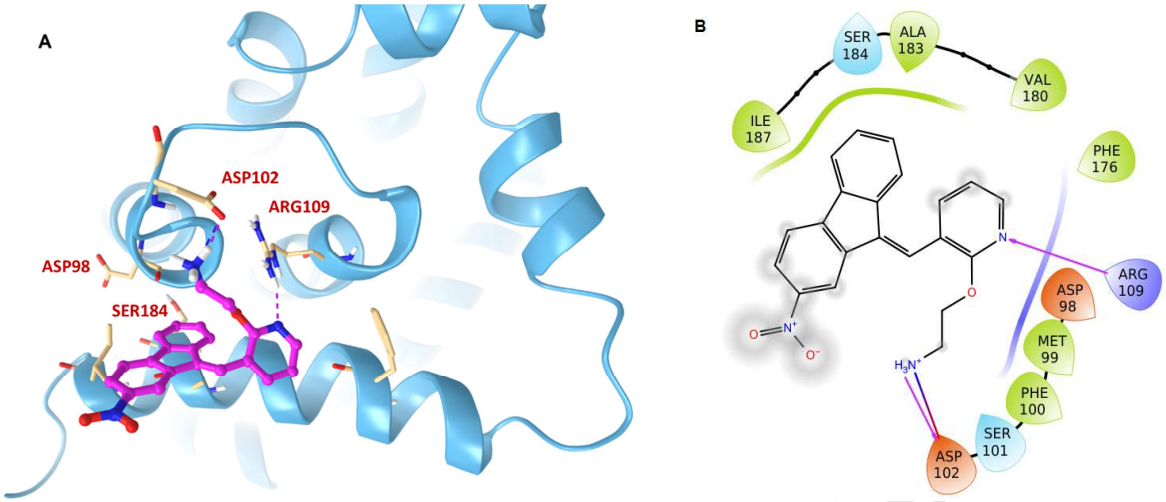

Fig. 2. (A) Predicted binding mode of compound **49** (magenta) docking into S184 site binding pocket of Bax protein (blue ribbon). Key residues of binding site are shown in yellow sticks. Hydrogen bonds are depicted as dashed purple lines, and salt bridge is shown in dashed blue line. (B) Interaction diagram of binding site between compound **49** and the Bax protein.

*2.2.3 The Inhibitory Activities of Compound **49** (**CYD-4-61**) against a Variety of BC Cells.*

To investigate whether our Bax activators retain efficacy in several breast cancer cell lines, the most potent compound **49** was evaluated for its growth inhibitory activity against two ER^+ BC cell lines (T47D and MCF-7), two TNBC cell lines (MDA-MB-231 and MDA-MB-468), Adriamycin (ADR)-resistant BC cell line MCF-7 as well as immortal mammary epithelial cell line (MCF-10A) at the indicated concentrations using MTT assays [41]. As shown in **Fig. 3** and **Table 3**, compound **49** was found to significantly inhibit the growth of ER^+ and TNBC cell lines, and the growth-inhibitory rate was greater than 50% at 1 μM with submicromolar to nanomolar IC_{50} values, which were more potent than those of **SMBA1** and **14** (**CYD-2-11**). Notably, compound **49** inhibited the growth of drug-resistant MCF-7 cells in a dose-dependent manner

(**Fig. 3**, bottom right panel), indicating Bax activation is a promising approach of overcoming breast cancer chemoresistance.

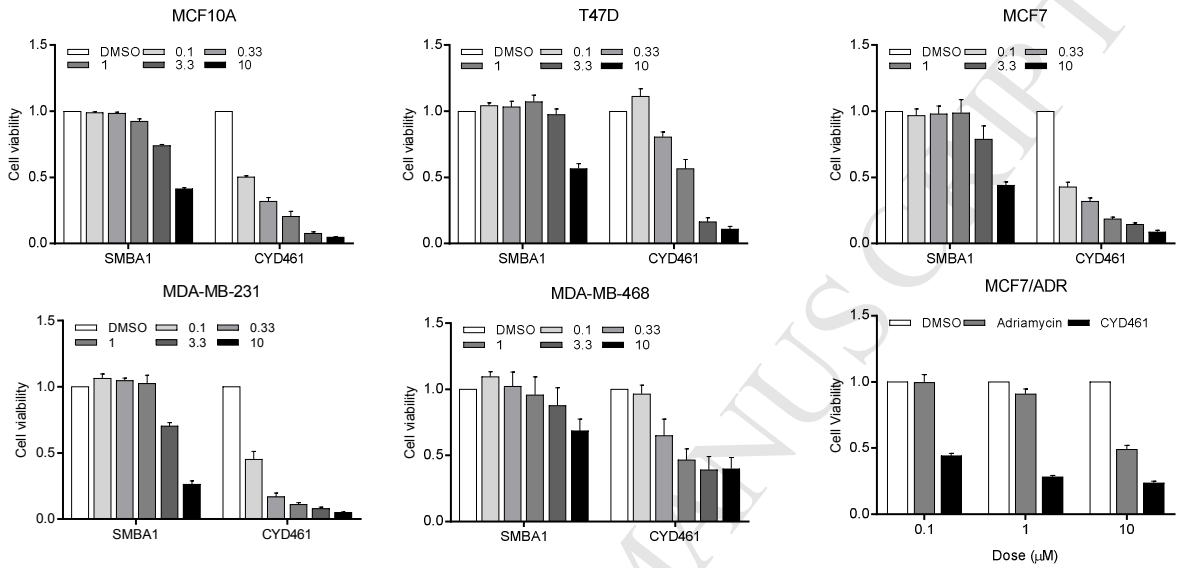

Fig. 3. Growth-inhibitory effect of **49** against various breast cancer cells. Breast cell lines were treated with **49** at indicated concentrations for 72 h. The values are the mean ± SE of at least three independent experiments.

Table 3. The antiproliferative effects of **SMBA1**, **14** (**CYD-2-11**) and **49** (**CYD-4-61**) against various cell lines.[a, b]

Compound	(IC_{50}, μM)				
	MCF-10A	T47D	MCF-7	MDA-MB-231	MDA-MB-468
SMBA1	7.58 ± 0.20	10.44 ± 0.38	8.30 ± 1.44	5.60 ± 0.69	16.12 ± 11.09
14	4.37 ± 0.74	9.47 ± 0.42	3.81 ± 0.76	3.22 ± 0.49	8.73 ± 2.89
49	0.11 ± 0.02	1.20 ± 0.35	0.06 ± 0.03	0.07 ± 0.03	1.61 ± 1.04

[a]Software: MasterPlex ReaderFit 2010, MiraiBio, Inc. [b]The values are the mean ±SE of at least three independent experiments.

*2.2.4 Effects of Compound **49** (**CYD-4-61**) on Colony Formation and Apoptosis Induction in BC Cells.*

Considering the potent antiproliferative activities against MCF-7 and MDA-MB-231 BC cell lines, we further evaluated the effect of compound **49** on the clonogenicity of cancer cells [42]. The colony formation assay was performed with **49** at a 1 μM concentration, as shown in **Figs. 4A-B**, and resulted in significantly blocking the clonogenic ability of both BC cells and almost no colony formation was observed following the addition of **49**. Hoechst nuclear staining was subsequently employed to verify if compound **49** was able to induce cancer cell apoptosis. As shown in **Fig. 4C**, compound **49** generated an increase of apoptotic cells as detected by the concentrated dense granular fluorescence compared to untreated cells, whereas no relevant apoptosis was detectable in control cells.

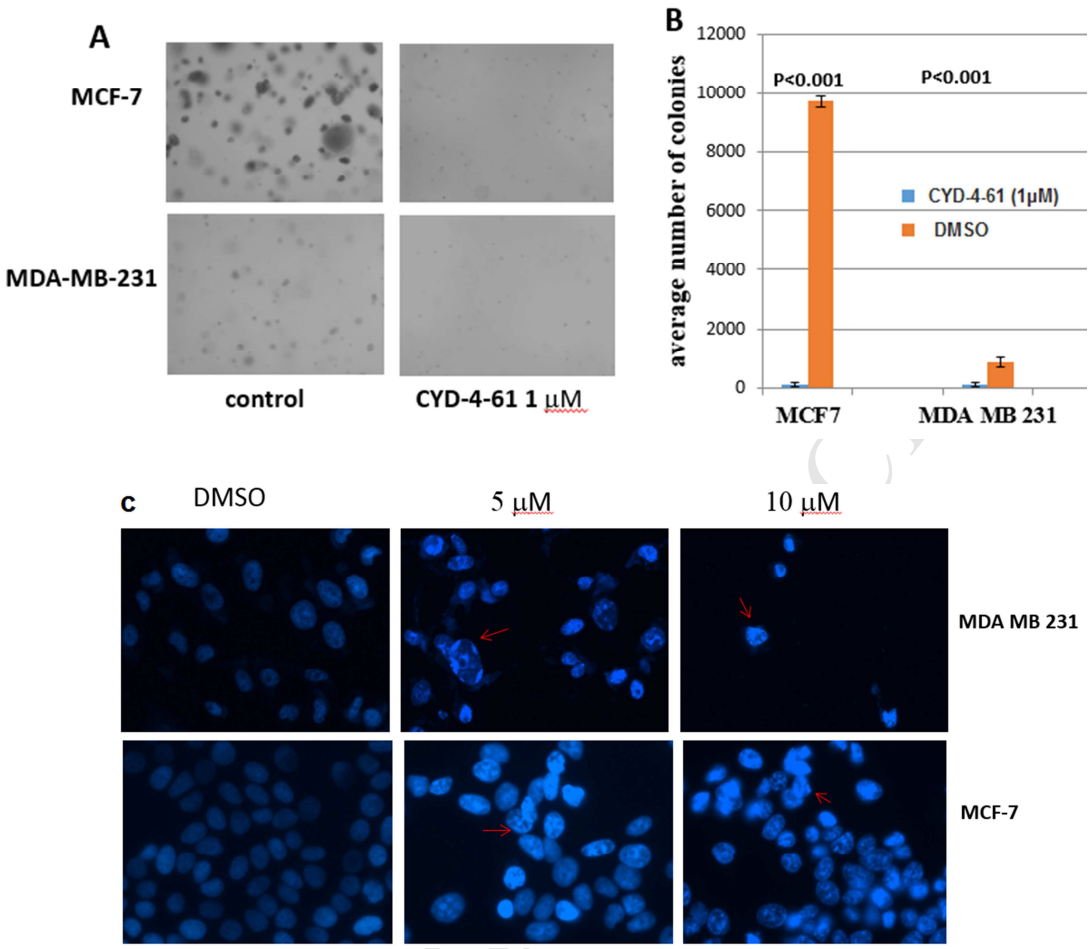

Fig. 4. Effects of compound **49** on colony formation and apoptosis in breast cancer cells. (A) **49** was used to treat MDA-MB-231 and MCF-7 cancer cells at 1 µM as indicated. Culture areas were scanned and digitally quantified with GelCount instrument. (B) Density data from scanning the stained culture areas were graphed as shown. Error bars represent standard deviations ($p < 0.001$). (C) Hoechst nuclear staining of MDA-MB-231 and MCF-7 to show the level of cells with apoptotic bodies by treated with **49** at 5 µM and 10 µM.

*2.2.5 Effects of Compound **49** (**CYD-4-61**) on Apoptosis-related Biomarkers.*

For illuminating the effects of our compounds on the expression of Bax protein in cancer cell, we directly measured the levels of the Bax active form (6A7) and the p-Bax induced by

compound **49**. As shown in **Fig. 5A**, levels of p-Bax were reduced in a time-dependent fashion in MCF-7 cells and the active Bax (6A7) isoform could be continuously observed through the 48 h treatment, while the total Bax protein level was increased after the treatment of **49**. Furthermore, dose-dependent increases for cytochrome *c* and decreasing levels of Bax protein were detected in cytosolic fractions for both MCF-7 and MDA-MB-231 after the addition of **49** at 5 μM concentration (**Fig. 5B**). This result suggests that Bax activation by **49** results in mitochondrial outer membrane permeabilization, thereby leading to cytochrome *c* release from mitochondria into the cytoplasm. To elucidate the potential mechanisms contributing to apoptosis, the expression levels of several protein markers related to apoptosis were determined by Western blotting analysis [43, 44]. As shown in **Fig. 5C**, treatment of MDA-MB-231 and MCF-7 with **49** dose-dependently led to the upregulation of cleaved PARP-1, cleaved caspase 3, and downregulation of cyclin D1. This data clearly demonstrates that the antiproliferative effect of compound **49** may be attributed to its induction of active Bax protein to trigger the intrinsic apoptotic signaling pathway, the mode of action which is consistent with our previously reported Bax activators [32, 33].

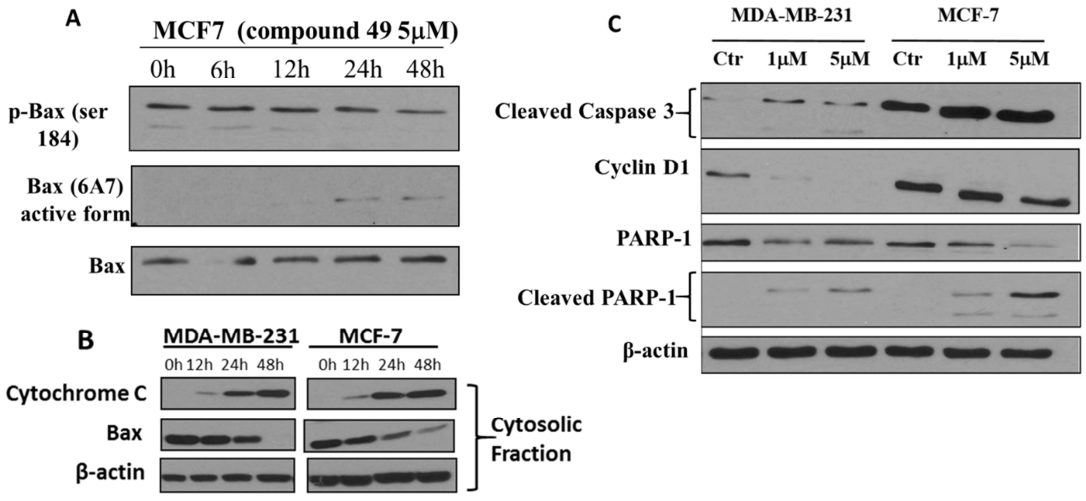

Fig. 5. Bax activation-mediated intrinsic apoptosis mechanism studies on compound **49**. (a) Effects of compound **49** on Bax active form (6A7) and inactive p-Bax. MCF-7 was treated with **49** (5 μM) and the p-Bax, active Bax (6A7) and total Bax levels were determined through 0-48 h by Western blot analysis. (B) Western-blot analysis of apoptotic biomarkers in cytosolic fraction after the treatment with **49** (5 μM) through 0-48 h. (C) Western blot analysis of apoptotic biomarkers induced by **49** at various concentrations (48 h).

*2.2.6 In Vivo Anticancer Efficacy of Compounds **14** (**CYD-2-11**) and **49** (**CYD-4-61**).*

To evaluate whether the promising *in vitro* anticancer activities of our compounds could be translated into *in vivo* antitumor efficacy for the proof-of-concept studies, we preliminarily examined the effects of compounds **14** and **49** in suppression of tumor growth in an aggressive triple-negative breast cancer MDA-MB-231 xenograft model [42]. SMBA1 was chosen as the positive control. As shown in **Fig. 6A**, compared to the vehicle control, compound SMBA1 was found to significantly suppress the growth of MDA-MB-231 tumors following intraperitoneal injection (i.p.) administration at a dose and regimen of 40 mg/kg once daily for 7 consecutive days, with an inhibition rate of 51%, and compound **14** at a half-dose level of SMBA1 exhibited a comparable inhibition rate (57%). Importantly, compound **49** at a very low dose of 2.5 mg/kg/day once daily exhibited significant *in vivo* efficacy with an inhibition rate of 55%. As depicted in **Fig. 6B**, slight body weight loss was observed for compound **49** in the treatment groups with potentially higher toxicity than SMBA1 and compound **14** (CYD-2-11), but within the tolerable range at the testing dose. The notable *in vivo* efficacy suggests that compounds **14** and **49** are improved lead compounds for further structural optimization and preclinical development. In addition, appropriate formulation and/or drug delivery strategies applicable to

compound **49** (e.g. nanoparticle encapsulation) are expected to further enhance the therapeutic and safety window.

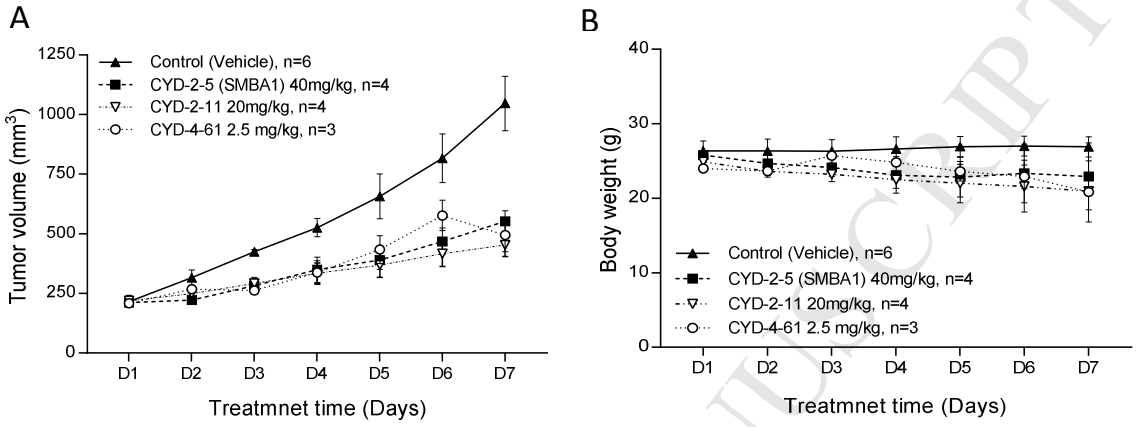

Fig. 6. *In vivo* efficacy of compounds **14** and **49** in comparison with the lead **SMBA1** in inhibiting growth of MDA-MB-231 xenograft tumors in mice (ip). (A) Data are presented as the mean ± SD of tumor volume at each time point. Significant differences between compounds **14**, **49**, **SMBA1** treatment group, and control were determined using one way ANOVA. $p \leqslant 0.05$. (B) Data showed mean ± SD of mouse body weight at each time point.

3. Conclusion

To identify potent Bax activators for breast cancer treatment, we have conducted a comprehensive structural optimization campaign based on our lead compound SMBA1 through several strategies, including the introduction of various alkylamino side chains to render deeper access to the S184 pocket, replacement of carbon atoms with nitrogen, and the reduction of the nitro group of 9*H*-fluorene scaffold. Diverse analogues were synthesized and evaluated for their antiproliferative effects against both triple-negative BC (e.g. MDA-MB-231 and MDA-MB-468)

and ER-positive BC (e.g. MCF-7 and T47D) cell lines. Among them, compounds **14** and **49** displayed improved potency against the these BC cell lines, especially **49**, which not only exhibited 80 to 130-fold enhancement of antiproliferative effects in both MDA-MB-231 and MCF-7 cancer cell lines with nanomolar IC_{50} values of 0.07 μM and 0.06 μM, respectively, but also displays the potential to overcome Adriamycin (ADR)-resistant MCF-7. Mechanism of action studies based on compound **49** suggest that it activates Bax protein by inhibiting its phosphorylation, resulting in mitochondrial outer membrane permeabilization, induction of cytochrome *c* release, and promotion of breast cancer cell apoptosis. Furthermore, compound **14** at 20 mg/kg and compound **49** at 2.5 mg/kg, respectively, showed significant tumor growth inhibition efficacy in a MDA-MB-231 tumor xenograft model compared to SMBA1 at a dose of 40 mg/kg. Further structural optimization based on compounds **14** and **49** to discover novel Bax activators with improved potency and safer toxicity profiles, as well as enhanced druggability for cancer treatment are ongoing.

4. Experimental protocols

4.1 Chemistry

All reactions were performed in glassware containing a stir bar and the commercially available starting materials and all the commercial available chemical reagents and solvents were reagent grade and used without further purification. The reactions were performed under an air atmosphere unless otherwise stated. Preparative column chromatography was performed using silica gel 60 and a particle size of 0.063−0.200 mm (70−230 mesh, flash). Analytical TLC was carried out employing silica gel 60 F254 plates (Merck, Darmstadt, Germany). Visualization of the developed chromatograms was performed with detection by UV (254 nm). ^{1}H and ^{13}C spectra were recorded on a Bruker-600 (^{1}H, 300 MHz or 600 MHz; ^{13}C, 75 MHz or 150 MHz;

^{19}F, 300 MHz) spectrometer with $CDCl_3$, $CDCl_3$ + CD_3OD or DMSO-*d6* as the solvent and TMS as an internal reference. Chemical shifts down-field from TMS were expressed in parts per million, and *J* values were given in hertz. Purity of final compounds was determined by analytical HPLC, which was carried out on a Shimadzu HPLC system (model: CBM-20A LC-20AD SPD-20AUV−vis). All biologically evaluated compounds are >95% pure.

*4.1.1 (E/Z)-9-(2-Bromobenzylidene)-2-nitro-9H-fluorene (**2**).*

To a solution of 2-nitrofluorene (422 mg, 2.0 mmol) and 2-bromobenzalhyde (370 mg, 2.0 mmol) in 10 mL of methanol was added KF-Al_2O_3 (320 mg, 2.0 mmol). The reaction mixture was stirred at 65 ^{o}C for 16 h, and then evaporated in vacuo. The residue was purified by silica gel column chromatography (ethyl acetate/CH_2Cl_2, 1:4) to give compound **2** as a yellow foam. Yield 401 mg, 53%. ^{1}H NMR (600 MHz, DMSO-d_6) δ 8.97 (d, *J* = 2.1 Hz, 1H), 8.35 (dd, *J* = 8.4, 2.1 Hz, 0.65H), 8.29 (dd, *J* = 8.4, 2.1 Hz, 0.35H), 8.19 – 8.16 (m, 1.65H), 8.10 (d, *J* = 7.6 Hz, 1H), 8.03 (s, 0.35H), 7.91 – 7.85 (m, 1.35H), 7.72 (d, *J* = 7.5 Hz, 0.35H), 7.66 (d, *J* = 7.5 Hz, 0.65H), 7.60 – 7.46 (m, 3.35H), 7.26 (t, *J* = 7.6 Hz, 0.65H), 7.10 (d, *J* = 7.9 Hz, 0.65H). ^{13}C NMR (150 MHz, DMSO-d_6) δ 147.61, 146.88, 146.76, 144.74, 140.25, 139.57, 138.99, 137.64, 137.06, 136.94, 136.52, 136.46, 135.54, 135.45, 133.48, 133.35, 131.68, 131.40, 131.18, 130.91, 130.37, 130.04, 129.94, 129.89, 129.54, 128.55, 125.01, 124.66, 124.35, 123.36, 123.13, 122.53, 122.24, 122.06, 121.47, 121.26, 119.10, 117.14. HRMS (ESI) calcd for $C_{20}H_{12}BrNO_2$, 378.0130 $[M + H]^+$; found, 378.0122.

*4.1.2 (E/Z)-2-((2-Nitro-9H-fluoren-9-ylidene)methyl)aniline (**4**).*

To a solution of **2** (189 mg, 0.5 mmol) in 5 mL of toluene was sequentially added diphenylmethanimine (99 mg, 0.55 mmol), $Pd_2(dba)_3$ (46 mg, 0.05 mmol), BINAP (31 mg, 0.05 mmol), and NaO*t*Bu (67 mg, 0.6 mmol) under N_2 atmosphere. The reaction mixture was stirred

at 110 ^{o}C for 18 h, and then evaporated *in vacuo*. The resulting residue was purified by silica gel column chromatography (MeOH/CH_2Cl_2, 1:40) to give compound **3** as a yellow solid. Yield 170 mg, 71%.

To a solution of **3** (143 mg, 0.3 mmol) in 8 mL of THF was added 2 mL of 1N HCl. The mixture was stirred at rt for 2 h and then adjusted to pH 8 by adding saturated $NaHCO_3$ solution and extracted with CH_2Cl_2 (3 × 10 mL). The combined organic layer was washed with water, dried over Na_2SO_4, filtered, and concentrated *in vacuo*. The residue was purified by silica column chromatography (MeOH/CH_2Cl_2, 1:10) to give the compound **4** as a yellow solid. Yield 87 mg, 92%. ^{1}H NMR (600 MHz, $CDCl_3$ + CD_3OD) δ 8.59 (d, J = 2.1 Hz, 0.4H), 8.29 (d, J = 2.1 Hz, 0.6H), 8.18 (dd, J = 8.3, 2.1 Hz, 0.4H), 8.11 (dd, J = 8.4, 2.1 Hz, 0.6H), 7.84 – 7.82 (m, 0.6H), 7.76 – 7.69 (m, 2H), 7.66 (s, 0.6H), 7.64 (s, 0.4H), 7.57 (dd, J = 7.9, 1.0 Hz, 0.4H), 7.42 – 7.30 (m, 2.6H), 7.25 – 7.15 (m, 1.4H), 6.84 – 6.77 (m, 2H). ^{13}C NMR (150 MHz, $CDCl_3$ + CD_3OD) δ 146.97, 146.69, 146.33, 144.66, 144.55, 140.53, 139.82, 138.56, 137.87, 136.84, 136.78, 135.25, 135.16, 130.47, 130.21, 130.09, 130.06, 128.97, 128.93, 128.81, 128.61, 126.57, 126.48, 124.85, 123.80, 123.45, 120.93, 120.89, 120.65, 120.61, 120.03, 119.62, 119.43, 118.58, 118.34, 116.07, 115.90, 115.87. HRMS (ESI) calcd for $C_{20}H_{15}N_2O_2$, 315.1134 $[M + H]^+$; found, 315.1125.

*4.1.3 (E/Z)-N^1,N^1-Dimethyl-N^2-(2-((2-nitro-9H-fluoren-9-ylidene)methyl)phenyl)ethane-1,2-diamine (**5**).*

To a solution of **2** (189 mg, 0.5 mmol) in 5 mL of toluene was sequentially added N^1,N^1-dimethylethane-1,2-diamine (53 mg, 0.6 mmol), $Pd_2(dba)_3$ (46 mg, 0.05 mmol), BINAP (31 mg, 0.05 mmol), and NaO*t*Bu (67 mg, 0.6 mmol) under N_2 atmosphere. The reaction mixture was stirred at 110 ^{o}C for 18 h, and then evaporated *in vacuo*. The resulting residue was purified by

silica gel column chromatography (MeOH/CH_2Cl_2, 1:10) to give compound **5** as a yellow solid. Yield 56 mg, 29%. ^{1}H NMR (600 MHz, $CDCl_3$) δ 8.71 (d, J = 2.1 Hz, 0.35H), 8.46 (d, J = 2.1 Hz, 0.65H), 8.31 (dd, J = 8.3, 2.1 Hz, 0.35H), 8.24 (dd, J = 8.4, 2.1 Hz, 0.65H), 7.95 – 7.93 (m, 0.65H), 7.86 – 7.82 (m, 2H), 7.75 – 7.71 (m, 1.35H), 7.52 – 7.47 (m, 1.7H), 7.45 – 7.41(m, 1.3H), 7.40 – 7.36 (m, 0.65H), 7.26 (td, J = 7.6, 1.1 Hz, 0.35H), 6.89 – 6.61 (m, 2H), 4.53 (brs, 1H), 3.29 – 3.27 (m, 2H), 2.56 – 2.52 (m, 2H), 2.17 (s, 2.1H), 2.15 (s, 3.9H). ^{13}C NMR (150 MHz, $CDCl_3$) δ 147.15, 146.88, 146.52, 146.36, 146.17, 144.46, 140.90, 140.10, 138.57, 138.19, 137.02, 136.87, 135.11, 135.03, 130.92, 130.59, 130.43, 130.33, 128.90, 128.76, 128.47, 126.93, 126.73, 124.99, 123.73, 123.41, 120.96, 120.91, 120.76, 120.54, 120.30, 119.62, 119.41, 117.09, 116.85, 115.99, 111.29, 111.18, 57.92, 45.12, 41.35, 41.18. HRMS (ESI) calcd for $C_{24}H_{24}N_3O_2$, 386.1869 $[M + H]^+$; found, 386.1859.

*4.1.4 (E/Z)-9-(2-Methoxybenzylidene)-2-nitro-9H-fluorene (**6**).*

To a solution of 2-nitrofluorene (211 mg, 1.0 mmol) and *o*-anisaldehyde (272 mg, 2.0 mmol) in 5 mL of methanol was added KF-Al_2O_3 (160 mg, 1.0 mmol). The reaction mixture was stirred at 65 ^{o}C for 16 h, and then evaporated in vacuo. The residue was purified by silica gel column chromatography (ethyl acetate/CH_2Cl_2, 1:2) to provide compound **6** as a yellow foam. Yield 155 mg, 47%. ^{1}H NMR (300 MHz, $CDCl_3$) δ 8.70 (d, J = 2.1 Hz, 0.4H), 8.49 (d, J = 2.1 Hz, 0.6H), 8.30 – 8.21 (m, 1H), 7.94 – 7.77 (m, 4H), 7.69 (d, J = 7.5 Hz, 0.4H), 7.62 (dd, J = 7.5 Hz, 0.6H), 7.53 – 7.38 (m, 2.6H), 7.23 (t, J = 7.8 Hz, 0.4H), 7.15 – 7.04 (m, 2H), 3.93 and 3.91 (s, 3H). ^{13}C NMR (75 MHz, $CDCl_3$) δ 157.82, 157.69, 147.11, 146.73, 146.46, 144.38, 141.13, 140.37, 138.83, 138.25, 137.16, 136.81, 134.38, 134.18, 131.00, 130.91, 130.71, 128.83, 128.79, 128.55, 128.41, 127.15, 124.50, 124.20, 123.66, 123.33, 121.00, 120.82, 120.61, 120.34, 119.79,

119.52, 119.47, 116.09, 111.12, 110.92, 55.55, 55.51. HRMS (ESI) calcd for $C_{21}H_{16}NO_3$, 330.1130 $[M + H]^+$; found, 330.1121.

*4.1.5 (E/Z)-2-(2-((2-Nitro-9H-fluoren-9-ylidene)methyl)phenoxy)ethan-1-ol (**8**).*

To a solution of compound **7** (158 mg, 0.5 mmol) in 5 mL of DMF was added NaH (40 mg, 1.0 mmol). After stirred at rt for 20 min, 2-bromoethan-1-ol (125 mg, 1.0 mmol) was added and the reaction was stirred at 80 ^oC for 24 h. Water (20 mL) was added and the reaction was extracted with CH_2Cl_2 (3 × 10 mL). The combined organic layer was washed with water, dried over Na_2SO_4, filtered, and concentrated in vacuo. The residue was purified by silica column chromatography (MeOH/CH_2Cl_2, 1:20) to give compound **8** as a yellow oil. Yield 136 mg, 68%. ^1H NMR (600 MHz, DMSO-d_6) δ 8.85 (d, J = 2.1 Hz, 0.5H), 8.34 (d, J = 2.1 Hz, 0.5H), 8.32 (d, J = 2.0 Hz, 0.5H), 8.27 (dd, J = 8.4, 2.1 Hz, 0.5H), 8.17 – 8.15 (m, 1.5H), 8.11 – 8.08 (m, 2H), δ 7.64 – 7.61 (m, 1.5H), 7.54 – 7.51 (m, 1.5H), 7.47 (q, J = 7.4 Hz, 1H), 7.29 (t, J = 7.6 Hz, 0.5H), 7.25 – 7.21 (m, 1H), 7.12– 7.07 (m, 1H), 4.86 (t, J = 5.7 Hz, 0.5H), 4.82 (t, J = 5.6 Hz, 0.5H), 4.12 – 4.10 (m, 2H), 3.69 – 3.64 (m, 2H). ^{13}C NMR (150 MHz, $CDCl_3$) δ 156.68, 156.63, 147.11, 146.72, 146.45, 144.42, 140.99, 140.19, 138.80, 138.19, 137.05, 136.84, 134.65, 131.19, 131.01, 130.69, 128.96, 128.66, 128.59, 126.68, 124.86, 124.55, 124.52, 123.83, 123.47, 121.22, 121.10, 121.01, 120.93, 120.81, 119.82, 119.63, 119.58, 116.12, 112.46, 112.26, 77.25, 77.04, 76.83, 69.87, 69.78, 61.37, 61.33. HRMS (ESI) calcd for $C_{22}H_{18}NO_4$, 360.1236 $[M + H]^+$; found, 360.1226.

*4.1.6 (E/Z)-9-(2-(2-Fluoroethoxy)benzylidene)-2-nitro-9H-fluorene (**9**).*

Compound **7** (158 mg, 0.5 mmol) was dissolved in 5 mL of THF and colded to 0 ^oC under ice bath, then DIAD (182 mg, 0.9 mmol) was added. After stirred at 0 ^oC for 20 min, the 2-fluoroethan-1-ol (58 mg, 0.9 mmol) and Ph_3P (236 mg, 0.9 mmol) was added and the reaction

was stirred at rt for 16 h. Water (20 mL) was added and the reaction was extracted with CH_2Cl_2 (3 × 10 mL). The combined organic layer was washed with water, dried over Na_2SO_4, filtered, and concentrated *in vacuo*. The residue was purified by silica column chromatography (MeOH/CH_2Cl_2, 1:10) to give the compound **9** as a yellow foam. Yield 110 mg, 61%. ^{1}H NMR (600 MHz, DMSO-d_6) ^{1}H NMR (600 MHz, DMSO-d_6) δ 8.82 (d, J = 2.1 Hz, 0.5H), 8.32 – 8.24 (m, 1.5H), 8.15 – 8.03 (m, 3.5H), 7.64 – 7.60 (m, 1H), 7.56 – 7.45 (m, 3H), 7.29 – 7.25 (m, 1.5H), 7.17 – 7.11 (m, 1H), 4.75 – 4.63 (m, 2H), 4.39 – 4.32 (m, 2H). ^{13}C NMR (150 MHz, DMSO-d_6) δ 156.72, 147.39, 146.66, 146.53, 144.33, 140.87, 140.03, 138.71, 137.98, 136.79, 136.70, 134.31, 134.16, 131.56, 131.46, 131.36, 131.22, 129.71, 129.57, 129.28, 128.67, 128.03, 124.91, 124.48, 124.41, 124.25, 124.03, 122.30, 122.03, 121.61, 121.37, 121.12, 121.03, 119.22, 116.59, 113.41, 113.34, 82.73 (d, J = 167 Hz), 82.50 (d, J = 167 Hz), 68.24 (d, J = 18 Hz), 68.15 (d, J = 18 Hz). ^{19}F NMR (300 MHz, $CDCl_3$) δ -223.42 and -223.64. HRMS (ESI) calcd for $C_{22}H_{17}FNO_3$, 362.1192 $[M + H]^+$; found, 362.1234.

*4.1.7 (E/Z)-N-Methyl-2-(2-((2-nitro-9H-fluoren-9-ylidene)methyl)phenoxy)ethan-1-amine (**11**).*

Intermediate **10** was prepared by a procedure similar to that used to prepare compound **9**.

To a solution of the **10** (94 mg, 0.2 mmol) in 3 mL of CH_2Cl_2 was added TFA (456 mg, 4.0 mmol) and the mixture was stirred overnight at rt. The reaction was adjusted to pH 8 by adding saturated $NaHCO_3$ and was extracted with CH_2Cl_2 (3 × 10 mL). The combined organic layer was washed with water, dried over Na_2SO_4, filtered, and concentrated *in vacuo*. The residue was purified by silica column chromatography (MeOH/CH_2Cl_2, 1:10) to give compound **11** as a yellow foam. Two step yield 72 mg, 39%. ^{1}H NMR (600 MHz, $CDCl_3$) δ 8.65 (d, J = 2.1 Hz, 0.5H), 8.46 (d, J = 2.1 Hz, 0.5H), 8.24 (dd, J = 8.4, 2.1 Hz, 0.5H), 8.19 (dd, J = 8.4, 2.1 Hz, 0.5H), 7.90 – 7.86 (m, 1H), 7.86 (s, 0.5H), 7.81 – 7.77 (m, 2H), 7.71 – 7.69 (m, 0.5H), 7.64 –

7.63 (m, 0.5H), 7.60 (dt, *J* = 7.5, 1.4 Hz, 0.5H), 7.50 – 7.38 (m, 2H), 7.39 (td, *J* = 7.5, 1.0 Hz, 0.5H), 7.25 – 7.20 (m, 0.5H), 7.11 (td, *J* = 7.5, 1.0 Hz, 0.5H), 7.05 – 7.05 (m, 1.5H), 4.19 – 4.17 (m, 2H), 2.97 – 2.92 (m, 2H), 2.41 (s, 3H). ^{13}C NMR (150 MHz, $CDCl_3$) δ 156.99, 156.96, 147.07, 146.69, 146.37, 144.36, 141.09, 140.25, 138.71, 138.25, 137.11, 136.77, 134.41, 131.12, 131.07, 131.02, 130.71, 128.92, 128.87, 128.65, 128.49, 127.03, 126.95, 124.78, 124.57, 124.45, 123.70, 123.37, 121.01, 120.89, 120.74, 120.71, 119.78, 119.56, 119.51, 116.00, 112.40, 112.25, 67.93, 67.74, 50.62, 36.35, 36.26. HRMS (ESI) calcd for $C_{23}H_{21}N_2O_3$, 373.1552 $[M + H]^+$; found, 373.1545.

*4.1.8 (E/Z)-N,N-Dimethyl-2-(2-((2-nitro-9H-fluoren-9-ylidene)methyl)phenoxy)ethan-1-amine (**12**).*

Compound **12** was prepared in 51% yield (98 mg) by a procedure similar to that used to prepare compound **9**. The title compound was obtained as a yellow foam. ^{1}H NMR (600 MHz, $CDCl_3$) δ 8.63 (d, *J* = 2.1 Hz, 0.5H), 8.50 (d, *J* = 2.1 Hz, 0.5H), 8.22 (dd, *J* = 8.4, 2.1 Hz, 0.5H), 8.18 (dd, *J* = 8.4, 2.1 Hz, 0.5H), 7.91 (d, *J* = 10.7 Hz, 1H), 7.87 (d, *J* = 7.6 Hz, 0.5H), 7.79 – 7.75 (m, 2.5H), 7.68 (dd, *J* = 7.8, 1.7 Hz, 0.5H), 7.61 (ddd, *J* = 7.8, 1.7Hz, 0.5H), 7.47 – 7.42 (m, 2H), 7.38 (td, *J* = 7.4, 1.0 Hz, 0.5H), 7.24 – 7.20 (m, 0.5H), 7.11 (td, *J* = 7.5, 0.9 Hz, 0.5H), 7.08 – 7.04 (m, 1.5H), 4.21 – 4.18 (m, 2H), 2.75 (t, *J* = 6.0 Hz, 1H), 2.72 (t, *J* = 6.0 Hz, 1H), 2.34 (s, 3H), 2.31 (s, 3H). ^{13}C NMR (150 MHz, $CDCl_3$) δ 157.19, 157.10, 147.03, 146.64, 146.37, 144.27, 141.21, 140.39, 138.74, 138.24, 137.11, 136.72, 134.17, 134.03, 131.09, 131.01, 130.74, 128.87, 128.79, 128.56, 128.39, 127.30, 127.26, 124.83, 124.49, 124.45, 123.62, 123.26, 121.01, 120.84, 120.75, 120.65, 120.56, 119.74, 119.51, 119.49, 115.89, 112.27, 112.24, 67.21, 67.08, 58.13, 46.10, 46.07. HRMS (ESI) calcd for $C_{24}H_{23}N_2O_3$, 387.1709 $[M + H]^+$; found, 387.1700.

*4.1.9 Tert-butyl (E/Z)-(2-(2-((2-nitro-9H-fluoren-9-ylidene)methyl)phenoxy)ethyl)carbamate (**13**).*

Compound **13** was prepared in 55% yield (126 mg) by a procedure similar to that used to prepare compound **9**. The title compound was obtained as a yellow solid. ^{1}H NMR (600 MHz, $CDCl_3$) δ 8.71 (d, *J* = 2.1 Hz, 0.5H), 8.47 (d, *J* = 2.1 Hz, 0.5H), 8.32 (dd, *J* = 8.4, 2.1 Hz, 0.5H), 8.25 (dd, *J* = 8.4, 2.1 Hz, 0.5H), 7.95 – 7.93 (m, 0.5H), 7.90 – 7.84 (m, 3H), 7.71 – 7.69 (m, 0.5H), 7.66 (dt, *J* = 7.5, 1.1 Hz, 0.5H), 7.63 (dt, *J* = 7.5, 1.1 Hz, 0.5H), 7.51 – 7.42 (m, 2.5H), 7.25 (td, *J* = 7.5, 1.1 Hz, 0.5H), 7.15 (td, *J* = 7.5, 1.2 Hz, 0.5H), 7.10 – 7.05 (m, 1.5H), 4.79 and 4.74 (brs, 1H), 4.16 – 4.14 (m, 2H), 3.53 – 3.50 (m, 2H), 1.41 (s, 9H). ^{13}C NMR (150 MHz, $CDCl_3$) δ 156.68, 156.62, 155.82, 155.75, 147.19, 146.79, 146.45, 144.49, 141.10, 140.27, 138.81, 138.26, 137.11, 136.87, 134.61, 131.17, 131.04, 130.73, 128.96, 128.93, 128.64, 128.55, 126.77, 126.73, 124.81, 124.59, 124.47, 123.84, 123.48, 121.17, 121.08, 120.92, 120.83, 119.85, 119.63, 119.59, 116.11, 112.40, 112.20, 79.56, 67.89, 40.06, 28.33. HRMS (ESI) calcd for $C_{27}H_{27}N_2O_5$, 459.1920 $[M + H]^+$; found, 459.1913.

*4.1.10 (E/Z)-2-(2-((2-Nitro-9H-fluoren-9-ylidene)methyl)phenoxy)ethan-1-amine (**14**).*

Compound **14** was prepared in 66% yield (55 mg) by a procedure similar to that used to prepare compound **11**. The title compound was obtained as a yellow foam. ^{1}H NMR (600 MHz, $CDCl_3$) δ 8.60 (d, *J* = 2.1 Hz, 0.65H), 8.37 (d, *J* = 2.1 Hz, 0.35H), 8.20 (dd, *J* = 8.4, 2.1 Hz, 0.65H), 8.13 (dd, *J* = 8.4, 2.1 Hz, 0.35H), 7.86 – 7.82 (m, 0.7H), 7.79 (s, 0.65H), 7.75 – 7.73 (m, 2H), 7.60 (d, *J* = 7.9 Hz, 0.65H), 7.58 – 7.52 (m, 1H), 7.43 – 7.36 (m, 1.7H), 7.33 (t, *J* = 7.4 Hz, 0.65H), 7.15 (t, *J* = 7.6 Hz, 0.65H), 7.05 (t, *J* = 7.5 Hz, 0.35H), 7.02 – 6.97 (m, 1.65H), 4.04 – 4.02 (m, 2H), 2.98 – 2.95 (m, 2H), 2.60 (brs, 2H). ^{13}C NMR (150 MHz, $CDCl_3$ + CD_3OD) δ 156.68, 147.01, 146.57, 146.40, 144.38, 140.93, 140.13, 138.66, 138.16, 137.01, 136.70, 134.46,

131.07, 131.02, 130.94, 130.64, 128.90, 128.85, 128.57, 128.49, 126.73, 124.66, 124.49, 124.34, 123.68, 123.37, 120.99, 120.92, 120.85, 120.74, 120.67, 119.68, 119.57, 119.52, 115.94, 112.20, 112.03, 69.94, 40.90, 40.82. HRMS (ESI) calcd for $C_{22}H_{19}N_2O_3$, 359.1396 $[M + H]^+$; found, 359.1393.

*4.1.11 (E/Z)-N-(2-(2-((2-Nitro-9H-fluoren-9-ylidene)methyl)phenoxy)ethyl)acetamide (**15**).*

To a solution of the **14** (72 mg, 0.2 mmol) in 3 mL of CH_2Cl_2 was added acetyl chloride (0.3 mmol) and Et_3N (404 mg, 0.4 mmol). The reaction was stirred at rt for 18 h, and then evaporated in vacuo and purified by silica gel column chromatography (CH_2Cl_2/MeOH, 1:20) to provide the compound **15** as a yellow solid. Yield 66 mg, 83%. ^{1}H NMR (300 MHz, $CDCl_3$) δ 8.69 (d, J = 2.1 Hz, 0.65H), 8.41 (t, J = 2.1 Hz, 0.35H), 8.29 (dt, J = 8.4, 2.1 Hz, 0.65H), 8.22 (dt, J = 8.4, 2.1 Hz, 0.35H), 7.94 – 7.81 (m, 3.35H), 7.64 – 7.58 (m, 1.65H), 7.52 – 7.40 (m, 2.35H), 7.26 – 7.22 (m, 0.65H), 7.17 – 7.03 (m, 2H), 5.69 (brs, 1H), 4.17 – 4.12 (m, 2H), 3.63 – 3.57 (m, 2H), 1.80 and 1.78 (s, 3H). ^{13}C NMR (75 MHz, $CDCl_3$) δ 170.15, 170.08, 156.44, 156.39, 147.20, 146.79, 146.38, 144.39, 140.14, 138.77, 138.19, 137.06, 136.82, 134.73, 131.08, 131.06, 130.97, 130.71, 129.05, 129.00, 128.74, 128.67, 126.72, 126.63, 124.78, 124.60, 123.84, 123.54, 121.36, 121.13, 121.10, 120.96, 120.75, 119.78, 119.69, 119.60, 116.01, 112.59, 112.26, 67.48, 38.92, 22.99. HRMS (ESI) calcd for $C_{24}H_{21}N_2O_4$, 401.1501 $[M + H]^+$; found, 401.1495.

*4.1.12 (S,E/Z)-3-Methyl-1-(2-((2-nitro-9H-fluoren-9-ylidene)methyl)phenoxy)butan-2-amine (**17**).*

Compound **17** was prepared in 39% yield (78 mg) by a procedure similar to that used to prepare compound **11**. The title compound was obtained as a yellow foam. ^{1}H NMR (600 MHz, $CDCl_3$) δ 8.62 (t, J = 2.4 Hz, 0.4H), 8.44 (d, J = 2.4 Hz, 0.6H), 8.22 (dt, J = 8.4, 2.7 Hz, 0.4H), 8.16 (dt, J = 8.4, 2.7 Hz, 0.6H), 7.88 – 7.84 (m, 1.6H), 7.80 – 7.74 (m, 2H), 7.68 (dd, J = 8.0, 2.7 Hz, 0.4H), 7.61 – 7.57 (m, 1H), 7.46 – 7.35 (m, 2.4H), 7.20 (td, J = 7.8, 3.0 Hz, 0.6H), 7.11 –

7.00 (m, 2 H), 4.11 – 4.03 (m, 1H), 3.90 – 3.86 (m, 1H), 2.93 – 2.89 (m, 1H), 1.75 – 1.67 (m, 1H), 0.94 – 0.93 (m, 6H). ^{13}C NMR (150 MHz, $CDCl_3$) δ 157.05, 157.02, 147.08, 146.68, 146.37, 144.35, 141.07, 140.24, 138.71, 138.25, 137.09, 136.76, 134.39, 130.99, 130.97, 130.94, 130.65, 128.91, 128.85, 128.62, 128.47, 126.88, 126.84, 124.77, 124.58, 124.42, 123.68, 123.36, 121.01, 120.88, 120.80, 120.65, 120.61, 119.80, 119.77, 119.57, 119.51, 115.90, 112.30, 112.16, 72.06, 55.89, 55.81, 30.94, 19.37, 18.11, 18.08. HRMS (ESI) calcd for $C_{25}H_{25}N_2O_3$, 401.1865 $[M + H]^+$; found, 401.1857.

*4.1.13 (S,E/Z)-1-(2-((2-Nitro-9H-fluoren-9-ylidene)methyl)phenoxy)butan-2-amine (**19**).*

Compound **19** was prepared in 33% yield (64 mg) by a procedure similar to that used to prepare compound **11**. The title compound was obtained as a yellow foam. ^{1}H NMR (300 MHz, $CDCl_3$) δ 8.67 (d, J = 2.1 Hz, 0.5H), 8.47 (d, J = 2.1 Hz, 0.5H), 8.30 – 8.20 (m, 1H), 7.91 – 7.80 (m, 3.5H), 7.71 – 7.60 (m, 1.5H), 7.51 – 7.38 (m, 2.5H), 7.23 (t, J = 7.6 Hz, 0.5H), 7.14 – 7.03 (m, 2H), 4.07 – 4.01 (m, 1H), 3.85 (t, J = 8.2 Hz, 1H), 3.10 – 2.99 (m, 1H), 1.62 – 1.27 (m, 4H), 0.99 – 0.93 (m, 3H). ^{13}C NMR (75 MHz, $CDCl_3$) δ 157.00, 156.96, 147.16, 146.75, 146.38, 144.41, 141.08, 140.27, 138.74, 138.30, 137.15, 136.81, 134.49, 134.46, 130.99, 130.95, 130.62, 128.90, 128.85, 128.61, 128.47, 126.84, 126.79, 124.81, 124.62, 124.45, 123.70, 123.40, 121.00, 120.89, 120.85, 120.65, 119.85, 119.59, 119.52, 115.93, 112.36, 112.21, 73.48, 52.14, 52.06, 26.91, 26.90, 10.40. HRMS (ESI) calcd for $C_{24}H_{23}N_2O_3$, 387.1709 $[M + H]^+$; found, 387.1700.

*4.1.14 (R,E/Z)-3-Chloro-2-(2-((2-nitro-9H-fluoren-9-ylidene)methyl)phenoxy)propan-1-amine (**21**).*

Compound **21** was prepared in 52% yield (120 mg) by a procedure similar to that used to prepare compound **11**. The title compound was obtained as a yellow foam. ^{1}H NMR (600 MHz, $CDCl_3$) δ 8.66 (q, J = 1.9 Hz, 0.4H), 8.46 (d, J = 2.1 Hz, 0.6H), 8.25 (dq, J = 6.8, 2.1 Hz, 0.4H),

8.20 (dq, *J* = 8.4, 2.1 Hz, 0.6H), 7.95 (s, 1H), 7.91 – 7.89 (m, 1H), 7.81 – 7.77 (m, 2H), 7.68 – 7.64 (m, 1.4H), 7.50 – 7.44 (m, 2H), 7.41 – 7.39 (m, 0.6H), 7.25 – 7.21 (m, 0.4H), 7.18 – 7.15 (m, 1.6H), 7.12 (t, *J* = 7.5 Hz, 0.4H), 4.58 – 4.55 (m, 1H), 3.78 – 3.70 (m, 2H), 3.15 – 3.07 (m, 2H). ^{13}C NMR (150 MHz, $CDCl_3$) δ 155.82, 155.76, 147.12, 146.67, 146.55, 144.43, 141.00, 140.15, 138.85, 138.10, 136.96, 136.80, 134.67, 134.61, 131.45, 131.43, 131.03, 130.72, 129.02, 128.68, 128.64, 126.78, 126.72, 126.29, 125.95, 124.52, 123.87, 123.53, 121.99, 121.83, 121.13, 120.93, 120.80, 119.64, 116.06, 114.90, 114.81, 80.16, 80.08, 43.03, 43.01, 42.94, 42.81. HRMS (ESI) calcd for $C_{23}H_{20}ClN_2O_3$, 407.1162 $[M + H]^+$; found, 407.1154.

*4.1.15 (E/Z)-4-(2-((2-Nitro-9H-fluoren-9-ylidene)methyl)phenoxy)piperidine (**23**).*

Compound **23** was prepared in 52% yield (103 mg) by a procedure similar to that used to prepare compound **11**. The title compound was obtained as a yellow foam. ^{1}H NMR (600 MHz, $CDCl_3$) *δ* 8.58 (d, *J* = 2.1 Hz, 0.45H), 8.40 (d, *J* = 2.1 Hz, 0.55H), 8.19 (dd, *J* = 8.4, 2.1 Hz, 0.45H), 8.13 (dd, *J* = 8.4, 2.1 Hz, 0.55H), 7.86 – 7.82 (m, 1.1H), 7.80 (s, 0.45H), 7.74 – 7.71 (m, 2H), 7.62 – 7.56 (m, 1.45H), 7.43 – 7.31 (m, 2.55H), 7.15 (t, *J* = 7.6 Hz, 0.45H), 7.07 – 6.98 (m, 2H), 5.54 (brs, 1H), 4.54 – 7.50 (m, 1H), 3.08 – 3.00 (m, 2H), 2.83 – 2.75 (m, 2H), 2.04 – 2.01 (m, 2H), 1.80 – 1.76 (m, 2H). ^{13}C NMR (150 MHz, $CDCl_3$) *δ* 155.29, 147.10, 146.61, 146.42, 144.33, 140.99, 140.13, 138.73, 138.15, 136.99, 136.69, 134.42, 131.31, 130.80, 130.49, 128.96, 128.83, 128.50, 126.86, 125.97, 125.57, 124.48, 123.67, 123.36, 121.11, 120.98, 120.81, 120.63, 119.62, 119.51, 115.77, 114.19, 114.12, 72.38, 71.91, 42.25, 42.05, 30.37, 30.09. HRMS (ESI) calcd for $C_{25}H_{23}N_2O_3$, 399.1709 $[M + H]^+$; found, 399.1705.

*4.1.16 (E/Z)-4-(2-(2-((2-Nitro-9H-fluoren-9-ylidene)methyl)phenoxy)ethyl)morpholine (**24**).*

Compound **24** was prepared in 82% yield (175 mg) by a procedure similar to that used to prepare compound **9**. The title compound was obtained as a yellow foam. ^{1}H NMR (600 MHz,

$CDCl_3$) δ 8.64 (d, J = 2.1 Hz, 0.55H), 8.41 (d, J = 2.2 Hz, 0.45H), 8.27 – 8.23 (m, 0.55H), 8.20 (dd, J = 8.3, 2.2 Hz, 0.45H), 7.87 – 7.84 (m, 1.45H), 7.83 – 7.77 (m, 2H), 7.67 (d, J = 7.9 Hz, 0.55H), 7.63 (dd, J = 7.6, 1.7 Hz, 0.55H), 7.58 (dd, J = 7.6, 1.7 Hz, 0.45H), 7.48 – 7.37 (m, 2.45H), 7.22 – 7.18 (m, 0.55H), 7.13 – 7.01 (m, 2H). 4.21 – 4.18 (m, 2H), 3.60 – 3.57 (m, 4H), 2.77 (t, J = 5.8 Hz, 1.1H), 2.71 (t, J = 5.7 Hz, 0.9H), 2.50 – 2.47 (m, 4H). ^{13}C NMR (150 MHz, $CDCl_3$) δ 156.92, 156.81, 147.09, 146.71, 146.34, 144.31, 141.02, 140.24, 138.72, 138.23, 137.14, 136.75, 134.42, 134.29, 130.88, 130.83, 130.57, 128.87, 128.79, 128.54, 128.47, 127.01, 124.87, 124.48, 123.65, 123.36, 120.97, 120.87, 120.65, 120.50, 119.77, 119.55, 119.47, 115.80, 112.28, 112.16, 66.81, 66.72, 57.42, 54.07. HRMS (ESI) calcd for $C_{26}H_{25}N_2O_4$, 429.1814 $[M + H]^+$; found, 429.1807.

*4.1.17 (E/Z)-1-(2-(2-((2-Nitro-9H-fluoren-9-ylidene)methyl)phenoxy)ethyl)piperidine (**25**).*

Compound **25** was prepared in 86% yield (183 mg) by a procedure similar to that used to prepare compound **9**. The title compound was obtained as a yellow foam. ^{1}H NMR (600 MHz, $CDCl_3$) δ 8.64 (d, J = 2.1 Hz, 0.5H), 8.49 (d, J = 2.1 Hz, 0.5H), 8.24 (dd, J = 8.3, 2.1 Hz, 0.5H), 8.19 (dd, J = 8.3, 2.1 Hz, 0.5H), 7.91 – 7.87 (m, 1.5H), 7.81 – 7.76 (m, 2.5H), 7.68 – 7.66 (m, 0.5H), 7.62 – 7.61 (m, 0.5H), 7.49 – 7.37 (m, 2H), 7.39 (t, J = 7.5 Hz, 0.5H), 7.22 (t, J = 7.6 Hz, 0.5H), 7.12 – 7.04 (m, 2H), 4.24 – 4.20 (m, 2H), 2.80 (dd, J = 7.1, 4.8 Hz, 1H), 2.75 (dd, J = 7.1, 4.9 Hz, 1H), 2.52 – 2.48 (m, 4H), 1.59 – 1.53 (m, 4H), 1.44 – 1.38 (m, 2H). ^{13}C NMR (150 MHz, $CDCl_3$) δ 157.16, 157.08, 147.04, 146.67, 146.37, 144.31, 141.19, 140.37, 138.73, 138.26, 137.15, 136.75, 134.20, 134.05, 130.99, 130.91, 130.72, 128.86, 128.79, 128.59, 128.40, 127.32, 127.29, 124.74, 124.50, 124.43, 123.64, 123.29, 121.01, 120.86, 120.71, 120.63, 120.48, 119.76, 119.53, 119.50, 115.88, 112.29, 112.13, 66.86, 66.78, 57.75, 57.74, 55.14, 55.08, 25.98, 24.10. HRMS (ESI) calcd for $C_{27}H_{27}N_2O_3$, 427.2022 $[M + H]^+$; found, 427.2015.

*4.1.18 (E/Z)-1-Methyl-4-(2-(2-((2-nitro-9H-fluoren-9-ylidene)methyl)phenoxy)ethyl)piperazine (**26**).*

Compound **26** was prepared in 73% yield (161 mg) by a procedure similar to that used to prepare compound **9**. The title compound was obtained as a yellow solid. ^{1}H NMR (600 MHz, $CDCl_3$) δ 8.61 (d, J = 2.2 Hz, 0.45H), 8.45 (d, J = 2.2 Hz, 0.55H), 8.23 (dd, J = 8.4, 2.2 Hz, 0.45H), 8.18 (dd, J = 8.4, 2.2 Hz, 0.55H), 7.88 – 7.82 (m, 1.55H), 7.79 – 7.75 (m, 2H), 7.72 (d, J = 7.9 Hz, 0.45H), 7.64 (d, J = 7.5 Hz, 0.45H), 7.59 (d, J = 7.4 Hz, 0.55H), 7.46 – 7.40 (m, 2H), 7.37 (t, J = 7.5 Hz, 0.45H), 7.20 (t, J = 7.6 Hz, 0.45H), 7.09 (t, J = 7.5 Hz, 0.55H), 7.07 – 7.01 (m, 1.55H), 4.21 – 4.19 (m, 2H), 2.80 (t, J = 5.8 Hz, 0.9H), 2.75 (t, J = 5.8 Hz, 1.1H), 2.58 – 2.39 (m, 8H), 2.26 and 2.24 (s, 3H). ^{13}C NMR (150 MHz, $CDCl_3$) δ 157.04, 156.94, 147.04, 146.65, 146.38, 144.29, 141.11, 140.30, 138.72, 138.22, 137.12, 136.72, 134.28, 134.12, 130.96, 130.91, 130.67, 128.91, 128.80, 128.58, 128.44, 127.17, 127.12, 124.80, 124.48, 124.44, 123.66, 123.32, 121.00, 120.87, 120.80, 120.62, 120.59, 119.76, 119.55, 119.50, 115.84, 112.26, 112.14, 77.36, 77.15, 76.94, 66.86, 66.73, 56.99, 56.91, 55.01, 53.56, 53.53, 45.95, 45.92. HRMS (ESI) calcd for $C_{27}H_{28}N_3O_3$, 442.2131 $[M + H]^+$; found, 442.2123.

*4.1.19 (E/Z)-1-(2-(2-((2-Nitro-9H-fluoren-9-ylidene)methyl)phenoxy)ethyl)piperazine (**28**).*

Compound **28** was prepared in 41% yield (88 mg) by a procedure similar to that used to prepare compound **11**. The title compound was obtained as a yellow solid. ^{1}H NMR (600 MHz, $CDCl_3$) δ 8.52 (d, J = 2.1 Hz, 0.6H), 8.32 (d, J = 2.1 Hz, 0.4H), 8.09 (dd, J = 8.4, 2.1 Hz, 0.6H), 8.06 (dd, J = 8.4, 2.1 Hz, 0.4H), 7.78 – 7.75 (m, 1.4H), 7.68 – 7.63 (m, 2H), 7.59 (d, J = 7.8 Hz, 0.6H), 7.54 (d, J = 7.5 Hz, 0.6H), 7.49 (d, J = 7.5 Hz, 0.4H), 7.39 – 7.26 (m, 2.4H), 7.10 (t, J = 7.6 Hz, 0.6H), 7.01 (t, J = 7.5 Hz, 0.4H), 6.99 – 6.91 (m, 1.6H), 4.76 (brs, 1H), 4.13 – 4.10 (m, 2H), 2.79 – 2.74 (m, 4H), 2.71 (t, J = 5.6 Hz, 1.2H), 2.66 (t, J = 5.6 Hz, 0.8H), 2.49 – 2.45 (m,

4H). ^{13}C NMR (75 MHz, $CDCl_3$) ***δ*** 156.92, 156.82, 147.10, 146.71, 146.38, 144.35, 141.04, 140.29, 138.74, 138.25, 137.16, 136.76, 134.44, 134.27, 130.96, 130.92, 130.85, 130.62, 128.94, 128.84, 128.59, 128.50, 127.06, 124.85, 124.51, 123.69, 123.39, 121.04, 120.94, 120.90, 120.70, 120.59, 119.80, 119.62, 119.53, 115.84, 112.29, 112.12, 77.45, 77.23, 77.03, 76.60, 66.73, 66.69, 57.34, 57.26, 53.45, 53.37, 45.16. HRMS (ESI) calcd for $C_{26}H_{26}N_3O_3$, 428.1974 $[M + H]^+$; found, 428.1968.

*4.1.20 (E/Z)-1-(4-(2-(2-((2-Nitro-9H-fluoren-9-ylidene)methyl)phenoxy)ethyl)piperazin-1-yl)ethan-1-one (**29**).*

Compound **29** was prepared in 77% yield (72 mg) by a procedure similar to that used to prepare compound **15**. The title compound was obtained as a yellow solid. ^{1}H NMR (600 MHz, $CDCl_3$) δ 8.57 (d, J = 2.1 Hz, 0.5H), 8.34 (d, J = 2.1 Hz, 0.5H), 8.18 (dd, J = 8.4, 2.1 Hz, 0.5H), 8.14 (dd, J = 8.4, 2.0 Hz, 0.5H), 7.82 – 7.80 (m, 1.5H), 7.76 – 7.72 (m, 2H), 7.62 (d, J = 7.9 Hz, 0.5H), 7.58 (d, J = 7.5 Hz, 0.5H), 7.53 (d, J = 7.5 Hz, 0.5H), 7.44 – 7.37 (m, 2H), 7.33 (t, J = 7.5 Hz, 0.5H), 7.15 (t, J = 7.6 Hz, 0.5H), 7.06 (t, J = 7.5 Hz, 0.5H), 7.02 – 6.97 (m, 1.5H), 4.17 – 4.03 (m, 2H), 3.47 – 3.45 (m, 2H), 3.27 – 3.19 (m, 2H), 2.75 (t, J = 5.5 Hz, 1H), 2.69 (t, J = 5.5 Hz, 1H), 2.47 – 2.38 (m, 4H), 1.94 and 1.92 (s, 3H). ^{13}C NMR (150 MHz, $CDCl_3$) δ 168.83, 168.74, 156.82, 156.70, 147.00, 146.65, 146.30, 144.29, 140.94, 140.17, 138.66, 138.14, 137.09, 136.72, 134.44, 134.22, 130.88, 130.81, 130.65, 128.93, 128.85, 128.62, 128.54, 127.01, 124.74, 124.44, 123.68, 123.37, 121.00, 120.94, 120.91, 120.71, 120.50, 119.73, 119.57, 119.51, 115.76, 112.22, 112.08, 66.82, 66.72, 56.86, 53.67, 53.57, 53.20, 53.09, 46.10, 41.26, 21.18. HRMS (ESI) calcd for $C_{28}H_{28}N_3O_4$, 470.2080 $[M + H]^+$; found, 470.2073.

*4.1.21 (E/Z)-1-(Methylsulfonyl)-4-(2-(2-((2-nitro-9H-fluoren-9-ylidene)methyl)phenoxy) ethyl)piperazine (**30**).*

To a solution of compound **28** (86 mg, 0.2 mmol) in 3 mL of CH_2Cl_2 was added methylsulfonyl chloride (35 mg, 0.3 mmol) and Et_3N (404 mg, 0.4 mmol). The reaction was stirred at rt for 4 h, and then evaporated in vacuo and purified by silica gel column chromatography (CH_2Cl_2/MeOH, 1:20) to provide compound **30** as a yellow solid. Yield 76 mg, 75%. ^{1}H NMR (600 MHz, $CDCl_3$) δ 8.59 (d, J = 2.1 Hz, 0.6H), 8.34 (d, J = 2.1 Hz, 0.4H), 8.21 (dd, J = 8.3, 2.1 Hz, 0.6H), 8.15 (dd, J = 8.3, 2.1 Hz, 0.4H), 7.83 – 7.80 (m, 1.4H), 7.78 – 7.75 (m, 2H), 7.64 (d, J = 7.9 Hz, 0.6H), 7.60 (dd, J = 7.6, 1.6 Hz, 0.6H), 7.55 – 7.53 (m, 0.4H), 7.45 – 7.34 (m, 2.4H), 7.17 (td, J = 7.6, 1.2 Hz, 0.6H), 7.08 (td, J = 7.5, 1.0 Hz, 0.4H), 7.05 – 6.97 (m, 1.6H), 4.16 – 4.13 (m, 2H), 3.07 (t, J = 5.1 Hz, 2.4H), 3.03 (t, J = 5.1 Hz, 1.6H), 2.77 (t, J = 5.5 Hz, 1.2H), 2.72 (t, J = 5.5 Hz, 0.8H), 2.66 and 2.63 (s, 3H), 2.55 – 2.52 (q, J = 5.5 Hz, 4H). ^{13}C NMR (150 MHz, $CDCl_3$) δ 156.84, 156.70, 147.10, 146.72, 146.35, 144.31, 140.94, 140.19, 138.72, 138.18, 137.13, 136.74, 134.55, 134.31, 130.91, 130.85, 130.81, 130.61, 128.99, 128.88, 128.60, 126.91, 124.96, 124.60, 124.44, 123.68, 123.42, 121.06, 120.95, 120.83, 120.51, 119.74, 119.66, 119.54, 115.71, 112.38, 112.33, 77.25, 77.04, 76.83, 66.80, 66.55, 56.59, 52.72, 52.67, 45.71, 34.19, 34.05. HRMS (ESI) calcd for $C_{27}H_{28}N_3O_5S$, 506.1750 $[M + H]^+$; found, 506.1743.

*4.1.22 (E/Z)-1-(Cyclopropylsulfonyl)-4-(2-(2-((2-nitro-9H-fluoren-9-ylidene)methyl)phenoxy) ethyl)piperazine (**31**).*

Compound **31** was prepared in 82% yield (87 mg) by a procedure similar to that used to prepare compound **30**. The title compound was obtained as a yellow solid. ^{1}H NMR (600 MHz, $CDCl_3$) δ 8.59 (s, 0.6H), 8.34 (s, 0.4H), 8.19 (d, J = 8.5 Hz, 0.6H), 8.15 (d, J = 8.4 Hz, 0.4H), 7.82 – 7.81 (m, 1.6H), 7.78 – 7.74 (m, 2H), 7.62 (d, J = 8.0 Hz, 0.6H), 7.59 (d, J = 7.7 Hz, 0.6H), 7.54 (d, J = 7.6 Hz, 0.4H), 7.45 – 7.33 (m, 2.4H), 7.16 (t, J = 7.7 Hz, 0.6H), 7.07 (t, J = 7.6 Hz, 0.4H), 7.03 – 6.98 (m, 1.6H), 4.16 – 4.13 (m, 2H), 3.15 – 3.15 (m, 4H), 2.78 – 2.72 (m, 2H), 2.54

– 2.52 (m, 4H), 2.15 – 2.09 (m, 1H), 1.06 – 1.02 (m, 2H), 0.87 – 0.83 (m, 2H). ^{13}C NMR (150 MHz, $CDCl_3$) δ 156.80, 156.69, 147.02, 146.65, 146.37, 144.30, 140.92, 140.15, 138.69, 138.15, 137.09, 136.71, 134.48, 134.29, 132.08, 132.01, 130.92, 130.89, 130.84, 130.64, 129.00, 128.88, 128.60, 126.94, 124.84, 124.42, 123.70, 123.41, 121.07, 121.00, 120.95, 120.80, 120.51, 119.73, 119.64, 119.56, 115.79, 112.24, 112.20, 66.81, 66.50, 56.66, 52.90, 45.99, 25.21, 25.11, 4.20. HRMS (ESI) calcd for $C_{29}H_{30}N_3O_5S$, 532.1906 $[M + H]^+$; found, 532.1902.

*4.1.23 (E/Z)-3-(2-((2-Nitro-9H-fluoren-9-ylidene)methyl)phenoxy)propan-1-amine (**33**).*

Compound **33** was prepared in 39% yield (72 mg) by a procedure similar to that used to prepare compound **11**. The title compound was obtained as a yellow foam. ^{1}H NMR (300 MHz, $CDCl_3$) δ 8.64 (d, J = 2.1 Hz, 0.4H), 8.44 (d, J = 2.1 Hz, 0.6H), 8.26 (dd, J = 8.4, 2.1 Hz, 0.4H), 8.19 (dd, J = 8.4, 2.1 Hz, 0.6H), 7.92 – 7.75 (m, 3.6H), 7.68 (d, J = 7.9 Hz, 0.4H), 7.64 – 7.57 (m, 1H), 7.49 – 7.36 (m, 2.6H), 7.20 (t, J = 7.6 Hz, 0.4H), 7.11 – 7.01 (m, 2H), 4.13 (t, J = 6.0 Hz, 2H), 2.79 (t, J = 6.8 Hz, 2H), 2.27 (s, 2H), 1.97 – 1.85 (m, 2H). ^{13}C NMR (75 MHz, $CDCl_3$ + CD_3OD) δ 166.60, 156.97, 156.92, 147.09, 146.67, 146.43, 144.41, 141.04, 140.25, 138.71, 138.26, 137.12, 136.74, 134.37, 134.32, 130.99, 130.93, 130.64, 128.92, 128.81, 128.56, 128.46, 126.95, 124.67, 124.51, 124.31, 123.67, 123.36, 121.00, 120.85, 120.74, 120.66, 120.52, 119.75, 119.58, 119.52, 115.90, 112.06, 111.97, 66.32, 66.28, 38.88, 38.72, 32.19, 32.09. HRMS (ESI) calcd for $C_{23}H_{21}N_2O_3$, 373.1552 $[M + H]^+$; found, 373.1543.

*4.1.24 (E/Z)-4-(2-((2-Nitro-9H-fluoren-9-ylidene)methyl)phenoxy)butan-1-amine (**35**).*

Compound **35** was prepared in 44% yield (85 mg) by a procedure similar to that used to prepare compound **11**. The title compound was obtained as a yellow foam. ^{1}H NMR (300 MHz, $CDCl_3$ + CD_3OD) δ 8.62 (d, J = 2.1 Hz, 0.5H), 8.42 (d, J = 2.1 Hz, 0.5H), 8.24 (dd, J = 8.4, 2.1 Hz, 0.5H), 8.17 (dd, J = 8.4, 2.1 Hz, 0.5H), 7.87 – 7.77 (m, 3.5H), 7.68 (d, J = 7.9 Hz, 0.5H),

7.62 – 7.54 (m, 1H), 7.45 – 7.33 (m, 2.5H), 7.18 (t, *J* = 7.6 Hz, 0.5H), 7.08 – 6.97 (m, 2H), 4.04 (t, *J* = 6.3 Hz, 2H), 3.06 (s, 2H), 2.67 (q, *J* = 6.7 Hz, 2H), 1.78 – 1.69 (m, 2H), 1.59 – 1.52 (m, 2H). ^{13}C NMR (75 MHz, $CDCl_3$ + CD_3OD) δ 157.02, 156.95, 147.03, 146.61, 146.40, 144.39, 141.06, 140.31, 138.65, 138.25, 137.15, 136.69, 134.25, 134.12, 130.98, 130.89, 130.64, 128.88, 128.77, 128.55, 128.42, 127.12, 127.08, 124.61, 124.49, 124.31, 123.60, 123.30, 120.96, 120.83, 120.62, 120.40, 119.74, 119.57, 119.48, 115.83, 112.12, 111.99, 67.96, 67.89, 40.83, 28.55, 26.39. HRMS (ESI) calcd for $C_{24}H_{23}N_2O_3$, 387.1709 $[M + H]^+$; found, 387.1700.

*4.1.25 (E/Z)-2-(2-(2-((2-Nitro-9H-fluoren-9-ylidene)methyl)phenoxy)ethoxy)ethan-1-amine (**37**).*

Compound **37** was prepared in 52% yield (105 mg) by a procedure similar to that used to prepare compound **11**. The title compound was obtained as a yellow foam. ^{1}H NMR (300 MHz, $CDCl_3$) δ 8.68 (d, *J* = 2.1 Hz, 0.45H), 8.46 (d, *J* = 2.1 Hz, 0.55H), 8.27 – 8.18 (m, 1H), 7.92 – 7.59 (m, 5H), 7.49 – 7.37 (m, 2.45H), 7.22 (t, *J* = 7.6 Hz, 0.55H), 7.14 – 7.04 (m, 2H), 4.26 – 4.22 (m, 2H), 3.84 – 3.76 (m, 2H), 3.57 – 3.48 (m, 2H), 2.85 – 2.76 (m, 2H), 2.20 (brs, 2H). ^{13}C NMR (75 MHz, $CDCl_3$) δ 157.10, 156.96, 147.09, 146.69, 146.37, 144.31, 141.11, 140.38, 138.75, 138.23, 137.15, 136.76, 134.35, 134.14, 131.08, 130.99, 130.93, 130.66, 128.89, 128.80, 128.56, 128.45, 127.21, 124.92, 124.58, 124.49, 123.65, 123.32, 121.01, 120.96, 120.85, 120.72, 120.69, 119.78, 119.54, 119.49, 115.98, 112.49, 112.41, 73.14, 69.32, 68.26, 68.10, 41.54. HRMS (ESI) calcd for $C_{24}H_{23}N_2O_4$, 403.1658 $[M + H]^+$; found, 403.1648.

*4.1.26 (E/Z)-2-(3-((2-Nitro-9H-fluoren-9-ylidene)methyl)phenoxy)ethan-1-amine (**41a**).*

3-Hydroxybenzaldehyde (61 mg, 0.5 mmol) was dissolved in 5 mL of THF and cooled to 0 ^{o}C under ice bath, and then DIAD (182 mg, 0.9 mmol) was added. After stirred at 0 ^{o}C for 20 min, *tert*-butyl (2-hydroxyethyl)carbamate (145 mg, 0.9 mmol) and Ph_3P (236 mg, 0.9 mmol) were added and the reaction was stirred at rt for 16 h. Water (20 mL) was added and the reaction

was extracted with CH_2Cl_2 (3 × 10 mL). The combined organic layer was washed with water, dried over Na_2SO_4, filtered, and concentrated *in vacuo*. The residue was purified by silica column chromatography (ethyl acetate/CH_2Cl_2, 1:2) to give the key intermediate **39a**.

To a solution of 2-nitrofluorene (63 mg, 0.3 mmol) and **39a** (80 mg, 0.3 mmol) in 5 mL of methanol was added KF-Al_2O_3 (48 mg, 0.3 mmol). The reaction mixture was stirred at 65 ^oC for 16 h, and then evaporated *in vacuo* to provide 105 mg of crude product **40a**. **40a** was then dissolved in 3 mL of CH_2Cl_2. TFA (456 mg, 4.0 mmol) was added and the mixture was stirred overnight at rt. Then the reaction was adjusted to pH 8 by adding saturated $NaHCO_3$ and was extracted with CH_2Cl_2 (3 × 10 mL). The combined organic layer was washed with water, dried over Na_2SO_4, filtered, and concentrated in vacuo. The residue was purified by silica column chromatography (MeOH/CH2Cl2, 1:10) to give the final compound **41a** as a yellow foam. Yield 61 mg, 85%. ^{1}H NMR (600 MHz, $CDCl_3$) δ 8.56 (d, J = 2.1 Hz, 0.5H), 8.48 (d, J = 2.1 Hz, 0.5H), 8.15 (dd, J = 8.3, 2.1 Hz, 0.5H), 8.11 (dd, J = 8.4, 2.1 Hz, 0.5H), 7.81 (dd, J = 7.8, 0.9 Hz, 0.5H), 7.78 – 7.75 (m, 0.5H), 7.74 – 7.70 (m, 1.5H), 7.69 – 7.68 (m, 0.5H), 7.67 (s, 0.5H), 7.64 (s, 0.5H), 7.52 – 7.49 (m, 2H), 7.42 – 7.39 (m, 1H), 7.36 (td, J = 7.5, 1.0 Hz, 0.5H), 7.21 (ddd, J = 7.9, 7.3, 1.2 Hz, 0.5H), 7.04 – 6.98 (m, 2H), 4.07 (t, J = 5.2 Hz, 2H), 3.16 – 3.14 (m, 2H), 1.54 (brs, 2H). ^{13}C NMR (150 MHz, $CDCl_3$) δ 159.70, 159.53, 146.89, 146.53, 146.31, 144.04, 141.17, 140.27, 138.70, 137.96, 136.70, 136.50, 133.25, 131.18, 131.11, 130.56, 130.44, 128.83, 128.77, 128.57, 128.30, 128.02, 127.74, 124.21, 123.54, 123.10, 121.05, 120.83, 120.33, 119.49, 119.46, 119.31, 115.52, 114.81, 114.61, 70.42, 70.35, 41.56. HRMS (ESI) calcd for $C_{22}H_{19}N_2O_3$, 359.1396 $[M + H]^+$; found, 359.1393.

*4.1.27 (E/Z)-2-(4-((2-Nitro-9H-fluoren-9-ylidene)methyl)phenoxy)ethan-1-amine (**41b**).*

Compound **41b** was prepared in 74% yield (53 mg) by a procedure similar to that used to prepare compound **41a**. The title compound was obtained as a yellow foam. ^{1}H NMR (600 MHz, $CDCl_3$) δ 8.47 (dd, J = 10.2, 2.3 Hz, 1H), 8.13 (dd, J = 8.4, 2.3 Hz, 0.5H), 8.08 (dd, J = 8.3, 2.2 Hz, 0.5H), 7.76 – 7.68 (m, 2.5H), 7.64 – 7.62 (m, 1.5H), 7.41 – 7.33 (m, 2.5H), 7.18 (t, J = 7.7 Hz, 0.5H), 7.14 – 7.09 (m, 2H), 7.02 – 6.97 (m, 1H), 4.04 – 4.00 (m, 2H), 3.2 – 3.09 (m, 2H), 1.57 (brs, 2H). ^{13}C NMR (150 MHz, $CDCl_3$) δ 159.24, 159.12, 146.94, 146.54, 144.35, 140.84, 139.99, 138.85, 137.78, 137.05, 136.74, 136.67, 136.57, 134.64, 134.62, 130.21, 130.07, 129.96, 129.83, 129.09, 128.96, 128.71, 128.68, 124.71, 123.88, 123.51, 121.99, 121.74, 121.06, 120.87, 120.54, 119.74, 119.51, 115.68, 115.64, 115.25, 115.05, 114.86, 70.50, 70.31, 41.60, 41.55. HRMS (ESI) calcd for $C_{22}H_{19}N_2O_3$, 359.1396 $[M + H]^+$; found, 359.1393.

*4.1.28 (E/Z)-2-((2-Amino-9H-fluoren-9-ylidene)methyl)phenol (**42**).*

To a solution of compound **7** (63 mg, 0.2 mmol) in 10 mL of THF was added 0.4 mL of sat. NH_4Cl and 0.4 mL of H_2O. Then Zinc powder (260 mg, 4.0 mmol) was added at 0 ^{o}C and the reaction was stirred at rt for 4 h. The Zinc solid was filtrated, and the filtrate was concentrated under vacuum to give a yellow residue, which was purified by silica gel column chromatography (MeOH/CH_2Cl_2, 1:5) to afford compound **42** as a yellow solid. Yield 31 mg, 55%. ^{1}H NMR (300 MHz, CD_3OD) δ 7.74 (d, J = 7.6 Hz, 0.65H), 7.63 (d, J = 6.6 Hz, 1H), 7.57 – 7.46 (m, 3.35H), 7.29 – 7.15 (m, 3H), 7.07 (d, J = 2.1 Hz, 0.65H), 6.96 – 6.87 (m, 2.35H), 6.78 – 6.70 (m, 1H). ^{13}C NMR (75 MHz, CD_3OD) δ 155.37, 155.33, 147.06, 146.33, 141.93, 141.22, 139.71, 139.15, 138.04, 136.13, 136.02, 132.28, 130.59, 130.14, 129.41, 129.35, 127.86, 127.47, 124.83, 124.27, 123.72, 122.91, 122.74, 119.73, 119.66, 119.62, 119.04, 118.88, 117.75, 117.58, 115.70, 115.36, 115.31, 115.28, 111.33, 107.00. HRMS (ESI) calcd for $C_{20}H_{16}NO$, 286.1232 $[M + H]^+$; found, 286.1225.

*4.1.29 (E/Z)-9-(2-(2-Aminoethoxy)benzylidene)-9H-fluoren-2-amine (**43**).*

Compound **43** was prepared in 63% yield (41 mg) by a procedure similar to that used to prepare compound **42**. The title compound was obtained as a yellow solid. ^{1}H NMR (300 MHz, $CDCl_3$) δ 7.71 (d, J = 7.5 Hz, 0.55H), 7.63 – 7.44 (m, 4H), 7.37 – 7.17 (m, 2.45H), 7.09 (d, J = 2.1 Hz, 0.45H), 7.03 – 6.89 (m, 2.55H), 6.69 – 6.59 (m, 1H), 4.04 – 3.99 (m, 2H), 3.05 – 2.96 (m, 2H), 2.43 (brs, 2H). ^{13}C NMR (75 MHz, $CDCl_3$) δ 156.88, 156.82, 146.01, 145.47, 141.77, 141.35, 139.74, 139.08, 138.41, 136.47, 136.34, 132.65, 131.22, 131.19, 130.70, 129.72, 129.69, 128.35, 128.01, 126.03, 125.34, 124.99, 124.14, 123.14, 122.92, 120.65, 120.60, 120.41, 120.11, 118.40, 118.28, 115.47, 115.31, 112.26, 111.18, 107.09, 70.75, 41.49. HRMS (ESI) calcd for $C_{22}H_{21}N_2O$, 329.1654 $[M + H]^+$; found, 329.1644.

*4.1.30 (E/Z)-3-((2-Nitro-9H-fluoren-9-ylidene)methyl)pyridin-2-ol (**44**).*

Conversion of 2-hydroxynicotinaldehyde to compound **44** was conducted by following procedures similar to that of preparation of compound **6** from **1**. The title compound was obtained as a yellow solid. Yield 30 mg, 47%. ^{1}H NMR (600 MHz, DMSO-d_6) δ 12.10 (brs, 1H), 8.76 (d, J = 2.2 Hz, 0.5H), 8.51 (d, J = 2.2 Hz,0.5H), 8.28 – 8.25 (m, 1H), 8.14 (t, J = 8.9 Hz, 1H), 8.10 – 8.02 (m, 1.5H), 7.98 – 7.93 (m, 1H), 7.87 – 7.83 (m, 1H), 7.79 (s, 0.5H), 7.62 (dd, J = 6.4, 2.1 Hz, 0.5H), 7.58 (dd, J = 6.5, 2.1 Hz, 0.5H), 7.51 – 7.45 (m, 1.5H), 7.39 – 7.33 (m, 0.5H), 6.41 – 6.37 (m, 1H). ^{13}C NMR (150 MHz, DMSO-d_6) δ 161.58, 147.35, 146.63, 146.58, 144.05, 142.59, 142.10, 140.89, 140.09, 138.76, 137.75, 137.51, 136.58, 136.48, 134.07, 133.82, 129.72, 129.53, 129.41, 129.22, 128.31, 127.88, 126.53, 126.33, 124.41, 124.32, 123.93, 122.36, 121.96, 121.55, 121.16, 120.99, 119.42, 116.49, 105.45. HRMS (ESI) calcd for $C_{19}H_{13}N_2O_3$, 317.0926 $[M + H]^+$; found, 317.0917.

*4.1.31 (E/Z)-2-Methoxy-3-((2-nitro-9H-fluoren-9-ylidene)methyl)pyridine (**45**).*

Conversion of 2-methoxynicotinaldehyde to compound **45** was conducted by following procedures similar to that for preparation of compound **6** from **1**. The title compound was obtained as a yellow solid. Yield 50 mg, 75%. ^{1}H NMR (300 MHz, $CDCl_3$) δ 8.69 (d, J = 2.1 Hz, 0.4H), 8.46 (d, J = 2.1 Hz, 0.6H), 8.35 – 8.23 (m, 2H), 7.99 – 7.68 (m, 5H), 7.52 – 7.41 (m, 1.6H), 7.25 – 7.23 (m, 0.4H), 7.10 – 7.01 (m, 1H), 4.07 (s, 3H). ^{13}C NMR (75 MHz, $CDCl_3$) δ 161.74, 161.70, 148.10, 147.81, 147.24, 146.73, 144.46, 140.80, 140.06, 139.31, 139.16, 139.08, 137.85, 136.89, 136.78, 135.42, 129.20, 129.01, 128.84, 128.68, 124.84, 124.71, 124.28, 124.06, 123.72, 121.22, 120.94, 120.90, 119.73, 119.64, 119.45, 118.81, 118.49, 116.60, 116.45, 116.18, 53.78. HRMS (ESI) calcd for $C_{20}H_{15}N_2O_3$, 331.1083 $[M + H]^+$; found, 331.1074.

*4.1.32 (E/Z)-3-((2-Nitro-9H-fluoren-9-ylidene)methyl)pyridin-2-amine (**47**).*

The synthesis of compound **47** was conducted by following procedures similar to that for preparation of compounds **4** from **1**. The title compound was obtained as a yellow solid. Yield 41 mg, 77%. ^{1}H NMR (600 MHz, DMSO-d_6) δ 8.89 (d, J = 2.1 Hz, 0.45H), 8.40 (d, J = 2.1 Hz, 0.55H), 8.32 – 8.27 (m, 1H), 8.16 – 8.08 (m, 3.5H), 7.94 (s, 0.45H), 7.86 (s, 0.55H), 7.76 – 7.71 (m, 1.45H), 7.56 – 7.48 (m, 1.55H), 7.40 – 7.32 (m, 0.45H), 6.73 – 6.68 (m, 1H), 6.32 (s, 2H). ^{13}C NMR (150 MHz, DMSO-d_6) $\boldsymbol{\delta}$ 158.14, 158.11, 150.09, 149.96, 147.22, 146.65, 146.58, 144.13, 141.03, 140.26, 138.77, 138.38, 137.82, 136.70, 136.53, 134.43, 134.18, 129.54, 129.40, 129.16, 128.28, 128.03, 124.36, 124.27, 123.86, 122.41, 122.14, 121.92, 121.21, 120.95, 119.15, 117.18, 114.09, 113.99, 112.38, 112.34. HRMS (ESI) calcd for $C_{19}H_{14}N_3O_2$, 316.1086 $[M + H]^+$; found, 316.1086.

*4.1.33 (E/Z)-2-((3-((2-Nitro-9H-fluoren-9-ylidene)methyl)pyridin-2-yl)oxy)ethan-1-amine (**49**).*

Conversion of *tert*-butyl (2-((3-formylpyridin-2-yl)oxy)ethyl)carbamate [37] to the final compound **49** was conducted by following procedures similar to that of preparation of

compounds **41a** from **39a**. The title compound was obtained as a yellow solid. Yield 61 mg, 85%. ^{1}H NMR (300 MHz, $CDCl_3$) δ 8.69 (d, J = 2.1 Hz, 0.5H), 8.44 (d, J = 2.1 Hz, 0.5H), 8.31 – 8.23 (m, 2H), 7.96 – 7.77 (m, 4.5H), 7.63 (d, J = 7.9 Hz, 0.5H), 7.50 – 7.43 (m, 1.5H), 7.25 – 7.22 (m, 0.5H), 7.09 – 7.02 (m, 1H), 4.51 – 4.47 (m, 2H), 3.12 – 3.05 (m, 2H), 1.72 (s, 3H). ^{13}C NMR (150 MHz, $CDCl_3$) δ 161.29, 161.25, 148.06, 147.77, 147.13, 146.66, 146.64, 144.42, 140.72, 139.90, 139.52, 139.44, 138.96, 137.81, 136.82, 136.68, 135.51, 135.41, 129.26, 129.08, 128.89, 128.73, 124.64, 124.51, 124.33, 124.07, 123.72, 121.23, 120.94, 120.89, 119.75, 119.65, 119.39, 118.77, 118.44, 116.74, 116.64, 116.12, 77.34, 77.13, 76.92, 68.80, 68.77, 41.38, 41.32. HRMS (ESI) calcd for $C_{21}H_{18}N_3O_3$, 360.1348 $[M + H]^+$; found, 360.1343.

*4.1.34 (E/Z)-1-(3-((2-Nitro-9H-fluoren-9-ylidene)methyl)pyridin-2-yl)piperazine (**50**).*

Conversion of 2-(piperazin-1-yl)nicotinaldehyde [38] to compound **50** was conducted by following procedures similar to that of preparation of compound **6** from **1**. The title compound was obtained as a yellow foam. Yield 58 mg, 61%. ^{1}H NMR (600 MHz, $CDCl_3$) δ 8.58 – 8.55 (m, 1H), 8.32 – 8.30 (m, 1H), 8.18 – 8.14 (m, 1H), 7.87 – 7.73 (m, 4H), 7.56 (s, 0.5H), 7.52 (s, 0.5H), 7.45 – 7.37 (m, 1.5H), 7.24 (t, J = 7.7 Hz, 0.5H), 6.91 – 6.87 (m, 1H), 3.32 – 3.30 (m, 4H), 2.92 – 2.89 (m, 4H). ^{13}C NMR (150 MHz, $CDCl_3$) δ 161.12, 161.10, 148.71, 148.55, 147.14, 146.66, 146.34, 144.13, 140.93, 140.05, 139.48, 138.69, 137.82, 136.63, 136.58, 133.20, 133.09, 129.16, 128.81, 128.68, 127.72, 124.21, 123.95, 123.50, 121.36, 121.04, 120.85, 120.45, 120.44, 119.85, 119.74, 119.28, 116.31, 116.20, 115.55, 51.42, 51.35, 46.33, 46.26. HRMS (ESI) calcd for $C_{23}H_{21}N_4O_2$, 385.1665 $[M + H]^+$; found, 385.1657.

*4.1.35 (E/Z)-1-Methyl-4-(3-((2-nitro-9H-fluoren-9-ylidene)methyl)pyridin-2-yl)piperazine (**51**).*

Conversion of 2-(4-methylpiperazin-1-yl)nicotinaldehyde [39] to compound **51** was conducted by following procedures similar to that of preparation of compound **6** from **1**. The title

compound was obtained as a yellow foam. Yield 70 mg, 73%. ^{1}H NMR (600 MHz, $CDCl_3$) δ 8.63 (d, J = 2.1 Hz, 0.45H), 8.61 (d, J = 2.1 Hz, 0.55H), 8.37 – 8.34 (m, 1H), 8.24 (dd, J = 8.4, 2.0 Hz, 0.45H), 8.22 (dd, J = 8.4, 2.1 Hz, 0.55H), 7.91 – 7.79 (m, 4H), 7.59 (s, 0.55H), 7.55 (s, 0.45H), 7.50 – 7.41 (m, 1.55H), 7.28 (td, J = 7.6, 1.2 Hz, 0.45H), 6.95 (dd, J = 7.5, 4.9 Hz, 0.55H), 6.92 (dd, J = 7.4, 4.8 Hz, 0.45H), 3.44 – 3.37 (m, 4H), 2.53 – 2.49 (m, 4H), 2.31 and 2.30 (s, 3H). ^{13}C NMR (75 MHz, $CDCl_3$) $\boldsymbol{\delta}$ 160.76, 148.76, 148.57, 147.31, 146.82, 146.40, 144.26, 140.99, 140.13, 139.59, 139.55, 138.79, 137.91, 136.73, 136.69, 133.36, 133.18, 129.17, 129.13, 128.81, 128.68, 127.78, 124.26, 124.01, 123.60, 121.35, 121.05, 120.86, 120.46, 120.37, 119.86, 119.78, 119.39, 116.31, 116.20, 115.68, 55.34, 55.24, 49.97, 49.93, 46.11, 46.08. HRMS (ESI) calcd for $C_{24}H_{23}N_4O_2$, 399.1821 $[M + H]^+$; found, 399.1818.

4.2 Molecular docking method.

The molecular docking study was performed with Small Molecule Drug Discovery Suite 2019-1 (Schrödinger, LLC, New York, NY, 2019). Solution structure of Bax (PDB ID: 1F16) was obtained from RCSB PDB bank and was preprocessed and optimized with Schrödinger Protein Preparation Wizard using default settings. The ligand was prepared with LigPrep to generate suitable 3-D conformation for docking. The grid (20 Å in size) was generated with Glide Grid and the grid center was selected at the center of residues of S184 site. Docking was conducted with Glide using SP mode. The docked results were visualized in Maestro and the best scoring poses were selected.

4.3 In vitro determination of newly synthesized compounds against cancer cell proliferation.

For IC_{50} calculations, breast cancer cell lines MCF-7, and MDA-MB-231 were seeded in 96-well plates at a density of 1×10^4 cells/well and treated with DMSO and 0.01, 0.1, 1, 5, 10, and 100 μM individual compound for 48 h, and then 20 μL of 3-(4,5-dimethylthiazol-2-yl)-2,5-

diphenyltetrazolium bromide (MTT) (5 mg/mL in PBS) was added to each well and further incubated for another 4 h, followed by adding 150 μL of DMSO to each well after removal of MTT solution. Absorbance was determined foe all wells by measuring OD at 550 nm after a 10 min incubation on a 96-well GlowMaxate absorbance reader (Promega, Madison, WI). Each individual compound was measured for designated concentrations in quadruplicate wells.

For cell viability assays for MCF-10A, MCF-7, T47D, MDA-MB-468, and MCF-7/ADR lines, the cells were seeded in 96-well plate at a density 1×10^3 cells/well. MDA-MB-231 cells were seeded at 600 cell/well. Each individual compound was measured for designated concentrations in quadruplicate wells and independently repeated three times.

4.4 Colony formation assay

Breast cancer MCF-7 and MDA-MB-231 cells were seeded in six-well tissue culture plates with a density of 800 cells per well and maintained in regular culture media. After 24 h, the cells were treated with compound **49** at 1 μM or DMSO as the vehicle. The culture media with the compounds were changed every 72 h. At the end of 2 weeks, the wells were washed twice with PBS buffer and 2 mL of 0.01% crystal violet staining buffer was added to each well and incubated for 10 min. The wells were then washed with PBS for 5 min for three times and allowed to dry. Photographs were then taken, and the density of the entire culture well area was digitally measured using the GelCount instrument (Oxford Optronix, U.K.). Experiments were performed in triplicate, and the density data were analyzed with one-way ANOVA using GraphPad Prizm 5 software package. Error bars represent standard deviation.

4.5 Western-blot analysis.

Breast cancer MCF-7 and MDA-MB-231 cells were treated with DMSO, or compounds **14** and **49**. After indicated time of treatment at designated doses, cells were harvested and lysed.

Protein concentrations were quantified by the method of Bradford with bovine serum albumin as the standard. Equal amounts of total cellular protein extract (30 μg) were separated by electrophoresis on SDS−polyacrylamide gels and transferred to PVDF membranes. After blocking with 5% nonfat milk, the membrane was incubated with the desired primary antibody overnight at the following dilutions: anti-Bax (1:1,000, ab32503), anti-pBax (1:500, Sigma SAB4504690), anti-Bax (6A7) (1:500, ENZO ALX-804-224-C100), anti-cytochrome C (1:1,000, CST11940), anti-PARP-1 (1:1,000, ab32138), anti-cleaved PARP-1 (1:1,000, CST5625), anti-cyclin D1 (1:1,000, CST2926), and β-actin (1:20,000, Sigma A5441). Subsequently, the membrane was incubated with appropriate secondary antibody. The immunoreactive bands were visualized by enhanced chemiluminescence (Thermo, 32106) as recommended by the manufacturer.

4.6 Hoechst staining for apoptosis detection in cells after CYD-4-61 treatment.

Breast cancer MCF-7 and MDA-MB-231 cells were incubated on coverslips in 12-well plates (2.5×10^5 cells/well). Cells were then treated with DMSO and CYD-4-61 at 5 and 10 μM for 24 h. Hoechst nuclear staining of MDA-MB-231 and MCF-7 was performed to show the level of cells with apoptotic bodies by treated with **49** at 5 μM and 10 μM. Cell were treated for 24 hour, then washed with 1X Binding Buffer twice. A 5 uL of FITC-annexin V, 5 uL of ethidium homodimer III and 5 uL of Hoechst 33342 was mixed into 100 uL 1X binding buffer to make the staining solution to stain each coverslip with the staining solution for 15 min. The coverslips were then mounted onto a slide with 1X binding buffer, residual 1X binding buffer was aspirated, and coverslip sealed with nail polish. Cells were observed for staining under a fluorescence microscope using a filter set for DAPI. Images were taken from center and

peripheral regions of the coverslips for analysis. An Apoptotic & Necrotic & Healthy Cells Quantification Kit (Biotium, Inc., CA. Cat #: 30018) was used for this assay.

4.7 In vivo antitumor activity determination.

All drugs were dissolved in 50% DMSO with 50% polyethylene glycol for *in vivo* administration. Body weights and tumor volumes were measured daily, and tumor volume was calculated according to the formula $V = 0.5 \times L \times W^2$, where L is length (mm) and W is width (mm). All procedures including mice and *in vivo* experiments were approved by the Institutional Animal Care and Use Committee (IACUC) of The University of Texas MD Anderson Cancer Center (MDACC). Female nude mice were obtained from MDACC Animal Core Facility and were used for orthotopic tumor studies at 6 weeks of age. The mice were maintained in a barrier unit with 12 h light−dark switch. Freshly harvested MDA-MB-231 cells (2.5×10^6 cells per mouse, resuspended in 100 μL of PBS) were injected into the fat pad of the third mammary gland of mice and then randomized into four groups. The mice were treated daily for 7 days with 40 mg/kg SMBA1, 20 mg/kg compound **14** (CYD-2-11), 2.5 mg/kg compound **49** (CYD-4-61), or vehicle through intraperitoneal injection, when the tumor volume reached 200 mm^3.

AUTHOR INFORMATION

Corresponding Author

*(J.Z.) Phone: (409) 772-9748; Fax: (409) 772-9818; E-mail: jizhou@utmb.edu.

*(Q.S.) Phone: (713) 834-6357; Fax: (713) 834-6350; E-mail: qshen@mdanderson.org.

Author Contributions

[1]These authors contributed equally to this work.

Notes

The authors declare no competing financial interest.

Acknowledgments

This work was supported by Breast Cancer Research Program (BCRP) Breakthrough Award W81XWH-17-1-0071 (to J.Z.) and W81XWH-17-1-0072 (to Q.S.) from the Department of Defense (DoD). We thank Drs. Lawrence C. Sowers and Tianzhi Wang for the NMR spectroscopy assistance.

Appendix A. Supplementary data

Supplementary data related to this article can be found at http://dx.doi.org/XXX

References

[1] L.A. Torre, F. Bray, R.L. Siegel, J. Ferlay, J. Lortet-Tieulent, A. Jemal, Global Cancer Statistics, 2012, CA Cancer J. Clin. 65 (2015) 87-108.

[2] N. Harbeck, M. Gnant, Breast cancer, The Lancet 389 (2017) 1134-1150.

[3] C.E. DeSantis, J. Ma, A. Goding Sauer, L.A. Newman, A. Jemal, Breast Cancer Statistics, 2017, Racial Disparity in Mortality by State, CA Cancer J. Clin. 67 (2017) 439-448.

[4] Z. Pan, Y. Chen, J. Liu, Q. Jiang, S. Yang, L. Guo, G. He, Design, synthesis, and biological evaluation of polo-like kinase 1/eukaryotic elongation factor 2 kinase (PLK1/EEF2K) dual inhibitors for regulating breast cancer cells apoptosis and autophagy, Eur. J. Med. Chem. 144 (2018) 517-528.

[5] E.B.C.T.C. Group, Effects of chemotherapy and hormonal therapy for early breast cancer on recurrence and 15-year survival: an overview of the randomised trials, The Lancet 365 (2005) 1687-1717.

[6] E.B.C.T.C. Group, Aromatase inhibitors versus tamoxifen in early breast cancer: patient-level meta-analysis of the randomised trials, The Lancet 386 (2015) 1341-1352.

[7] G. Schiavon, I.E. Smith, Status of adjuvant endocrine therapy for breast cancer, Breast Cancer Res. 16 (2014) 206.

[8] A.Y. Michaels, A.R. Keraliya, S.H. Tirumani, A.B. Shinagare, N.H. Ramaiya, Systemic treatment in breast cancer: a primer for radiologists, Insights Imaging 7 (2016) 131-144.

[9] E.A. Perez, Carboplatin in Combination Therapy for Metastatic Breast Cancer, The Oncologist 9 (2004) 518-527.

[10] L. Huang, Q. Liu, S. Chen, Z. Shao, Cisplatin versus carboplatin in combination with paclitaxel as neoadjuvant regimen for triple negative breast cancer, Onco. Targets. Ther. 10 (2017) 5739-5744.

[11] L. Ansari, F. Shiehzadeh, Z. Taherzadeh, S. Nikoofal-Sahlabadi, A.A. Momtazi-Borojeni, A. Sahebkar, S. Eslami, The most prevalent side effects of pegylated liposomal doxorubicin monotherapy in women with metastatic breast cancer: a systematic review of clinical trials, Cancer Gene. Ther. 24 (2017) 189-193.

[12] G. Gu, D. Dustin, S.A. Fuqua, Targeted therapy for breast cancer and molecular mechanisms of resistance to treatment, Curr. Opin. Pharmacol. 31 (2016) 97-103.

[13] W. Janni, Targeted Therapy of Breast Cancer, Oncol. Res. Treat. 39 (2016) 100-101.

[14] P. Samadi, S. Saki, F.K. Dermani, M. Pourjafar, M. Saidijam, Emerging ways to treat breast cancer: will promises be met? Cell Oncol. 41 (2018) 605-621.

[15] L. The, Breast cancer targeted therapy: successes and challenges, The Lancet 389 (2017) 2350.

[16] N.N. Danial, S.J. Korsmeyer, Cell Death: Critical Control Points, Cell 23 (2004) 205-219.

[17] Z. Liu, C. Wild, Y. Ding, N. Ye, H. Chen, E.A. Wold, J. Zhou, BH4 domain of Bcl-2 as a novel target for cancer therapy, Drug Discov. Today 21 (2016) 989-996.

[18] S.H. Kaufmann, D.L. Vaux, Alterations in the apoptotic machinery and their potential role in anticancer drug resistance, Oncogene 22 (2003) 7414-7430.

[19] Z. Liu, H. Chen, J. Zhou, Apoptosis Regulator BAX, In: S. Choi (eds), Encyclopedia of Signaling Molecules, Springer, New York, 2009, pp. 355-360

[20] Z. Liu, Y. Ding, N. Ye, C. Wild, H. Chen, J. Zhou, Direct Activation of Bax Protein for Cancer Therapy, Med. Res. Rev. 36 (2016) 313-341.

[21] M. Baltaziak, E. Duraj, M. Koda, A. Wincewicz, M. Musiatowicz, L. Kanczuga-Koda, M. Szymanska, T. Lesniewicz, B. Musiatowicz, Expression of Bcl-xL, Bax, and p53 in primary tumors and lymph node metastases in oral squamous cell carcinoma, Ann. N. Y. Acad. Sci. 1090 (2006) 18-25.

[22] J.A. Bush, G. Li, The role of Bcl-2 family members in the progression of cutaneous melanoma, Clin. Exp. Metastasis 20 (2003) 531-539.

[23] I. Milas, R. Komaki, T. Hachiya, R.S. Bubb, J.Y. Ro, L. Langford, R. Sawaya, J.B. Putnam, P. Allen, J.D. Cox, T.J. McDonnell, W. Brock, W.K. Hong, J.A. Roth, L. Milas, Epidermal Growth Factor Receptor, Cyclooxygenase-2, and BAX Expression in the Primary Non-Small Cell Lung Cancer and Brain Metastases, Clin. Cancer Res. 9 (2003) 1070-1076.

[24] Q. Sun, J. Hua, Q. Wang, W. Xu, J. Zhang, J. Zhang, J. Kang, M. Li, Expressions of GRP78 and Bax associate with differentiation, metastasis, and apoptosis in non-small cell lung cancer, Mol. Biol. Rep. 39 (2012) 6753-6761.

[25] A. Jansson, X.-F. Sun, Bax Expression Decreases Significantly From Primary Tumor to Metastasis in Colorectal Cancer, J. Clin. Oncol. 20 (2002) 811-816.

[26] I.R.K. Bukhlom, G. Bukholm, J.M. Nesland, Reduced expression of both Bax and Bcl-2 is independently associated with lymph node metastasis in human breast carcinomas, APMIS 110 (2002) 214-220.

[27] R.C. Bargou, C. Wagener, K. Bommert, M.Y. Mapara, P.T. Daniel, W. Arnold, M. Dietel, H. Guski, A. Feller, H.D. Royer, B. Dörken, Overexpression of the death-promoting gene bax-alpha which is downregulated in breast cancer restores sensitivity to different apoptotic stimuli and reduces tumor growth in SCID mice, J. Clin. Invest. 97 (1996) 2651-2659.

[28] A.J. Butt, S.M. Firth, M.A. King, R.C. Baxter, Insulin-like Growth Factor-binding Protein-3 Modulates Expression of Bax and Bcl-2 and Potentiates p53-independent Radiation-induced Apoptosis in Human Breast Cancer Cells, J. Biol. Chem. 275 (2000) 39174-39181.

[29] E. Gavathiotis, D.E. Reyna, J.A. Bellairs, E.S. Leshchiner, L.D. Walensky, Direct and selective small-molecule activation of proapoptotic BAX, Nat. Chem. Biol. 8 (2012) 639-645.

[30] M. Stornaiuolo, G. La Regina, S. Passacantilli, G. Grassia, A. Coluccia, V. La Pietra, M. Giustiniano, H. Cassese, S. Di Maro, D. Brancaccio, S. Taliani, A. Ialenti, R. Silvestri, C. Martini, E. Novellino, L. Marinelli, Structure-based lead optimization and biological evaluation of BAX direct activators as novel potential anticancer agents, J. Med. Chem. 58 (2015) 2135-2148.

[31] G. Zhao, Y. Zhu, C.O. Eno, Y. Liu, L. DeLeeuw, J.A. Burlison, J.B. Chaires, J.O. Trent, C. Lia, Activation of the Proapoptotic Bcl-2 Protein Bax by a Small Molecule Induces Tumor Cell Apoptosis, Mol. Cell. Biol. 34 (2014) 1198-1207.

[32] M. Xin, R. Li, M. Xie, D. Park, T.K. Owonikoko, G.L. Sica, P.E. Corsino, J. Zhou, C. Ding, M.A. White, A.T. Magis, S.S. Ramalingam, W.J. Curran, F.R. Khuri, X. Deng, Small-molecule Bax agonists for cancer therapy, Nat. Commun. 5 (2014) 4935.

[33] R. Li, C. Ding, J. Zhang, M. Xie, D. Park, Y. Ding, G. Chen, G. Zhang, M. Gilbert-Ross, W. Zhou, A.I. Marcus, S.Y. Sun, Z.G. Chen, G.L. Sica, S.S. Ramalingam, A.T. Magis, H. Fu, F.R.

Khuri, W.J. Curran, T.K. Owonikoko, D.M. Shin, J. Zhou, X. Deng, Modulation of Bax and mTOR for Cancer Therapeutics, Cancer Res. 77 (2017) 3001-3012.

[34] D. Villemin, M. Richard, Activation de la liasion C-H faiblement acide par adsorption sur KF-Al2O3, Tetrahedron Lett. 25 (1984) 1059-1060.

[35] G.A. Grasa, M.S. Viciu, J. Huang, S.P. Nolan, Amination Reactions of Aryl Halides with Nitrogen-Containing Reagents Mediated by Palladium/Imidazolium Salt Systems, J. Org. Chem. 66 (2001) 7729-7737.

[36] O. Mitsunobu, The use of diethyl azodicarboxylate and triphenylphosphine in synthesis and transformation of natural products, Synthesis 1 (1981) 1-28.

[37] X. Deng, J. Zhou, C. Ding, Preparation of fluoren-9-ylidenemethylpyridine derivatives as Bax agonists, WO2013028543.

[38] J.S. New, J.P. Yevich, J. Davis L. Temple, K.B. New, S.M. Gross, J. R. Francis Schlemmer, M.S. Bison, D.P. Taylor, L.A. Riblet, Atypical Antipsychotic Agents: Patterns of Activity in a Series of 3-Substituted 2-Pyridiny 1-1-piperazine Derivatives, J. Med. Chem. 31 (1998) 618-624.

[39] Brodney, M. Aaron, Pyridyl piperazines and their preparation and pharmaceutical compositions, for the treatment of CNS disorders or conditions that can be treated by serotonin-mediated neurotransmission, WO2006000912.

[40] Y. Ding, D. Li, C. Ding, P. Wang, Z. Liu, E.A. Wold, N. Ye, H. Chen, M.A. White, Q. Shen, J. Zhou, Regio- and Stereospecific Synthesis of Oridonin D-Ring Aziridinated Analogues for the Treatment of Triple-Negative Breast Cancer via Mediated Irreversible Covalent Warheads, J. Med. Chem. 61 (2018) 2737-2752.

[41] C. Ding, Y. Zhang, H. Chen, Z. Yang, C. Wild, L. Chu, H. Liu, Q. Shen, J. Zhou, Novel Nitrogen-Enriched Oridonin Analogues with Thiazole-Fused ARing: Protecting Group-Free

Synthesis, Enhanced Anticancer Profile, and Improved Aqueous Solubility, J. Med. Chem. 56 (2013) 5048-5058.

[42] C. Ding, Y. Zhang, H. Chen, Z. Yang, C. Wild, N. Ye, C.D. Ester, A. Xiong, M.A. White, Q. Shen, J. Zhou, Oridonin ring A-based diverse constructions of enone functionality: identification of novel dienone analogues effective for highly aggressive breast cancer by inducing apoptosis, J. Med. Chem. 56 (2013) 8814-8825.

[43] G. Liu, S. Song, X. Liu, A. Zhang, Z. Miao, C. Ding, Novel dihydroisoxazoline-alkyl carbon chain hybrid artemisinin analogues (artemalogs): synthesis and antitumor activities, RSC Adv. 6 (2016) 98975-98984.

[44] H. Chen, Z. Yang, C. Ding, A. Xiong, C. Wild, L. Wang, N. Ye, G. Cai, R.M. Flores, Y. Ding, Q. Shen, J. Zhou, Discovery of potent anticancer agent HJC0416, an orally bioavailable small molecule inhibitor of signal transducer and activator of transcription 3 (STAT3), Eur. J. Med. Chem. 82 (2014) 195-203.

Highlights:

- Novel analogues have been designed and synthesized based on Bax activator SMBA1.
- Compounds **14** (CYD-2-11) and **49** (CYD-4-61) showed enhanced anti-breast cancer activity compared to SMBA1.
- Compounds **14** and **49** displayed submicromolar to nanomolar IC_{50} values against breast cancer cell proliferation.
- Compounds **14** and **49** were identified to induce Bax-mediated apoptosis.
- Compounds **14** and **49** significantly suppressed breast cancer xenograft tumor growth *in vivo*.